A model of the interaction of T lymphocytes with electromagnetic waves.

Vincent Lauer

A model of the interaction of T lymphocytes with electromagnetic waves.

Vincent Lauer*

Abstract

This paper discusses a model of T lymphocytes and of their life-cycle which explains numerous experimental results that were generally considered as mutually incoherent. The interaction between a T Cell Receptor (TCR) and a peptide-Major Histocompatibility Complex (pMHC) is assumed to be based on a recognition mechanism, associated with negative thymus selection, and a non-recognition mechanism, associated with positive thymus selection. Each of these mechanisms is modelled using three quantum wells and transitions between these quantum wells naturally stimulated by the thermal electric field. Stimulation of the transitions with artificial electromagnetic waves in addition to the thermal background determines experimentally observed effects. The model is confronted to experimental results concerning in vivo or in vitro inhibition or stimulation of T lymphocytes by various types of waves, increased or decreased cancer growth rates, auto-immune effects and multi-generational studies on rats, and therapies including hyperthermia, the Lakhovsky "multiple waves oscillator" and the Priore systems.

1 Introduction

In quantum chemistry and biology, the energy of large macromolecules is usually considered as a function of the position of each atom within the molecule. The shape of a large macro-molecule is assumed to result from an energy minimization process, with the lowest energy state being the most stable. Molecules coming near to one another may react with each other, involving the undoing and re-building of chemical bonds. However, although the energy of the macro-molecule and the nature of the chemical bonds ultimately result from quantum mechanical calculations, it is possible to model them on a simplified, phenomenological basis. Most of the work by biologists is based on such simplified models which explicitly or implicitly hide the underlying quantum mechanics and allow an intuitive perception of implied phenomenons based on essentially classical (as opposite to quantum) considerations. For example, a biologist does not need quantum mechanical concepts to describe the immune system, despite the fact that all underlying mechanisms are ultimately described by quantum mechanics.

However, it becomes more and more apparent that some biological mechanisms involve specifically quantum phenomenons which cannot be modelled on a classical and phenomenological basis. For example, evidence of quantum coherence in photosynthesis has been found experimentally [23] [14] and a detailed explanation based on a known protein structure was later proposed [71]. Specifically quantum mechanisms have also been considered for explaining the avian compass [26] [44] or to explain certain biological effects of low-frequency electromagnetic waves [49] [5].

Thus, when experimental evidence points towards quantum mechanisms being implied in a biological phenomenon, such evidence should not be ignored. Further, if a specifically quantum mechanism plays a role in a biological phenomenon, as is most likely the case for photosynthesis, this cannot be ignored in the quest for understanding this phenomenon, because a classical and phenomenological view of biology may simply be unable to provide any consistent explanation.

This paper is based on the finding that basic properties of transitions between three quantum wells, applied to the TCR-pMHC recognition and combined with a model of the life-cycle of T cells which is in line with established knowledge, can explain experimentally observed effects of electromagnetic waves on T cells.

Unlike is the case in [23], the underlying quantum mechanism is not immediately apparent from well-known considerations, but instead requires more detailed preliminary explanations including its interaction with the full life-cycle of T cells (section 2). The experimental evidence (in the present case, resulting from re-analysis of a multiplicity of previously published results) then appears consistent in view of the proposed model, whilst it was previously viewed as incoherent [77]. Although the experimental results were essential in developing the model, for clarity the model (section 2) and experimental results (section 3) are separated in the paper.

Within the proposed model, the life-cycle of T cells described in section 2.1, is based on two mechanisms : a "recognition" (RE) mechanism associated to the recognition of antigens by the T cell, more specifically described in section 2.2 , and a "non-recognition" (NRE) mechanism associated to the non-recognition of antigens by the T cell and more specifically described in section 2.4. Both mechanisms are based on a quantum mechanical model involving transitions between quantum wells stimulated by thermal or artificial electromagnetic waves. The "recognition" mechanism yields inhibitory effects (INH) of radio-frequency electromagnetic waves (typically in the 0-3 GHz range) on the TCR-pMHC recognition (section 2.2.2), and stimulatory effects of waves above 9 GHz (ST, STM) on the same TCR-pMHC recognition(section 2.2.4). The "non-recognition" mechanism yields temporary inac-

*5 allée de l'Aire, 44240 La Chapelle sur Erdre, France
www.vincent-lauer.fr, contact@vincent-lauer.fr

tivation (INA) of T cells by radio-frequency electromagnetic waves typically in the 0-3 GHz range (section 2.4.3). The "recognition" mechanism is associated with negative thymus selection (section 2.2.3) and the "non-recognition" mechanism is associated with positive thymus selection (2.4.2) both of which heavily modify their overall effect on the immune system. Based on essentially the same model as the recognition mechanism, a detailed theory of fever and hyperthermia (FEV) is also discussed (section 2.3)). Different power densities, frequencies and bandwidths of a artificial waves yield different effects on immunity represented in multi-effects diagrams (section 2.5) and the application of these effects in practical cases is summarized in figure 8. The fundamental reason for which the immune system may have evolved towards this specific recognition mechanism is shortly discussed in section 2.7. Ancillary aspects which may impact the model are discussed in section 2.6 including a link between developmental timing parameters and the immune system (section 2.6.6) which is deduced from factual experimental observations discussed in section 3.1.4.

The application of the proposed model to experimental and statistical results is then discussed in the following order:

Effects of electromagnetic waves on the TCR-pMHC recognition below 3 GHz (section 3.1), including in vitro results on temporary inactivation (section 3.1.2) of T cells , experimental in vivo results on autoimmunity (section 3.1.3) and cancer (section 3.1.1), multigenerational studies on rats (section 3.1.4), cancer therapy with the Lakhovsky multiple wavelengths oscillator (section 3.1.11), decreased and increased cancer incidence in cellular phone users (sections 3.1.5 and 3.1.6), increases of cancer incidence near TV emitters (section 3.1.8), temporary increases of cancer at onset of cellular telephony base stations (section 3.1.7) or Television emitters (section 3.1.9), increase of melanoma incidence in relation to FM radio emitters (section 3.1.10).

Effects of electromagnetic waves on the TCR-pMHC recognition above 9 GHz (section 3.2), including experimental results with millimeter waves (section 3.2.1) , pathogen elimination with the Priore device (section 3.2.2) and experimental in vivo effects on T cells of a Priore-like exposure system (section 3.2.4).

Hyperthermia (section 3.3), including short-term anticancer and long-term pro-cancer effects of hyperthermia.

Further experiences are also proposed (section 4) to test aspects of the model.

Essential aspects of the mechanisms implied were first proposed in [48]. Conclusions in [48] relative to the influence on T cells and on diseases of low-power wideband electromagnetic waves are unmodified (see table "INH+ENS" in figure 8). However the model is improved by a more detailed analysis of transitions yielding a stimulatory (ST) effect at high frequencies and by the introduction of a specific Non-Recognition mechanism governing the reaction of a T cell to an antigen which is not recognized as its cognate antigen nor as a self antigen. These aspects yield a consistent interpretation of experimental results obtained at high power or low bandwidth. Amongst the situations already discussed in [48], they affect the interpretation of the increases of cancer incidence in heavy users of GSM [39] and the interpretation of the Lakhovsky multiple-waves oscillator [47]. Also, in the present paper the mathematical details of the underlying physics are only discussed to the extent which is necessary for understanding the experimental results, so as to avoid any un-necessary hypotheses.

2 The Model

Preliminary: this section uses a quantum mechanical approach based on general knowledge on quantum mechanics [12]. Treatment of the interaction of electromagnetic waves with matter is semi-classical : waves are treated classically and biological elements are treated as quantum systems, in a way which closely parallels the semi-classical theory of atom-field interaction [57].

2.1 Life-cycle of T cells

According to the model, each T cell (more specifically each T cell Receptor (TCR)) has an affinity for any antigen (p) presented on a Major Histocompatibility Complex (MHC). For example, this affinity may be characterized as $-\log\Omega_b$ wherein Ω_b is a Rabi frequency which will be defined in section 2.2. A second affinity may be defined as $-\log\Omega_{b'}$ wherein $\Omega_{b'}$ is a second Rabi frequency which will be defined in section 2.4. The interaction of the T cell with a presented antigen depends on its affinities with the antigen. If $-\log\Omega_b > -\log\Omega_{bmin}$ then a Recognition Mechanism (RE) is triggered. If $-Log\Omega_{b'} < -\log\Omega_{bmax}$ then a Non-Recognition Mechanism (NRE) is triggered. These mechanisms have different outcomes depending on the stage in the life-cycle of the T cell. The Recognition Mechanism (RE) yields Elimination of the T cell by Negative Selection (ENS) during negative selection in the "negative selection " section of the thymus; Proliferation during a primary or secundary immune reaction in a lymph node; and destruction (DES) of the antigen -presenting cell (APC) during interaction with an APC of the mature effector T cell in a diseased organ. The non-recognition mechanism (NRE) yields Elimination of the T cell by Positive Selection (EPS) during positive selection in the "positive selection" section of the thymus, and Temporary Inactivation (TI) during any of the Negative selection, Primary/secundary reaction, or interaction with an APC in a diseased organ. Figure 1 shows these steps of the life-cycle of a T cell.

In the model, the boundaries Ω_{bmin} and Ω_{bmax} are independent of the stage in the life-cycle of the T cell. This is essential, because:

(i) it allows positive selection to precisely select T cells which after thymus selection will not be temporarily inactivated when encountering self antigens (such T cells would be essentially useless).

(ii) it allows negative selection to select T cells which after thymus selection will not attack APCs presenting normal self antigens (such T cells would cause auto-immune diseases).

To ensure that Ω_{bmin} and Ω_{bmax} are independent of the stage in the life-cycle of the T cell, it is further as-

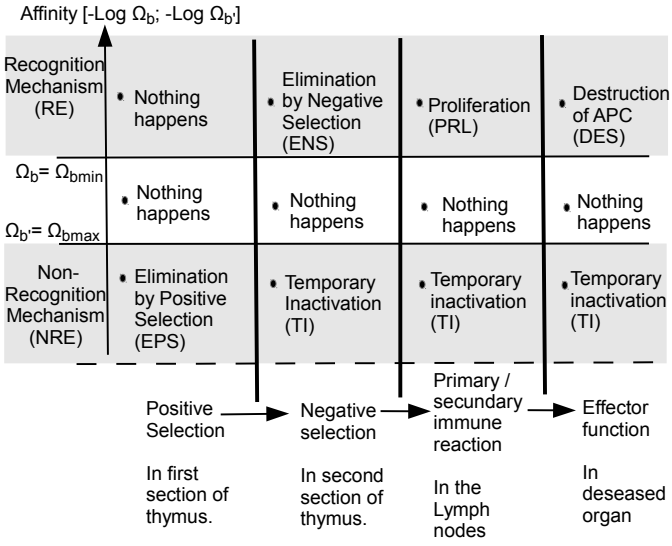

Figure 1: Life-cycle of T cells

sumed that the recognition (resp. non-recognition) mechanism is essentially common between the different stages of the life-cycle of the T cell, and that only the outcome of recognition (resp. non-recognition) differs between different stages.

The role of temporary inactivation in this model is as follows: when an effector T cell encounters an antigen which is not its cognate antigen and is not a normal antigen of the self, it has essentially met a potential threat which it is unable to overcome. Rather than staying by the threat, it is better for it to become temporarily inactivated so as to stop binding MHCs and thus be more easily evacuated to another area. This leaves the path open for other T cells to reach the threat. Temporary inactivation would thus be an essential mechanism for clearing an invaded area from any useless T cells and allowing T cells efficient against the threat to reach the area as soon as possible.

The existence and the role of temporary inactivation is in agreement with the findings in [80]. In [80] it was found that a T cell line needs both the correct MHC and the correct antigen to proliferate. This is the "recognition" case in which a naive T cell line recognizing its cognate antigen is induced in proliferating faster. It was also found that naive T cells transferred to host mice having the correct MHC but not the right antigen survive in a resting state. This resting state is interpreted in the present model as resulting from temporary inactivation of T cells following non-recognition of the antigen.

The non-recognition mechanism may operate in parallel or sequentially with the "recognition" mechanism . Generally, the exact manner in which the recognition and the non-recognition mechanisms are inter-related is unknown. However the two mechanisms are not independent because at the very least a T cell must not be temporarily activated when it recognizes its cognate antigen, which could potentially happen if the recognition and non-recognition mechanisms were independent. The most likely solution to this problem is to have $\Omega_b = \Omega_{b'}$. However at this stage there is uncertainty on this issue. For an easier understanding of the model one can assume $\Omega_b = \Omega_{b'}$, however there may be other arrangements yielding to essentially the same result.

Concerning the organization of the immune system, the model uses the known facts of positive and negative selection, and the generally accepted role of negative selection. It introduces temporary inactivation, and most importantly it introduces the idea of a stage-independent recognition mechanism and a stage-independent non-recognition mechanism.

2.2 Interaction mechanism for recognition of abnormal antigens by T cells (RE)

2.2.1 The "recognition" mechanism (RE)

In the present model, the recognition stage (RE) of the TCR-pMHC interaction can be modelled with a reasonable level of accuracy as three consecutive quantum wells (a), (b), (c) separated from each other by energy barriers as shown on figure 2. The entry of the TCR-pMHC system in well (c) is assumed to characterize recognition of the peptide p and from well (c) the TCR-pMHC system is assumed to always evolve towards destruction of the APC (in the case of CD8 T cells). Initial binding with the MHC may characterize well (a), with well (b) being an intermediate quantum well, however other arrangements are possible.

The dipole moments in quantum states (a),(b),(c) are assumed to differ from one another. It is shown in Appendix A that this condition generally results in the possibility of transitions between wells (a) and (b) and between wells (b) and (c) which are stimulated by electromagnetic waves. It is further shown in Appendix B that where the only electromagnetic wave present is the thermal background, in the radio-frequency domain these thermally stimulated transitions dominate over spontaneous decay, so that they represent the dominating transition mechanism between quantum wells (a) (b) and (c).

For the purpose of obtaining simple equations, I will first consider that there is only a single quantum state (respectively $|a\rangle, |b\rangle, |c\rangle$) in each well (resp. (a), (b), (c)) as shown in figure 3. The interaction picture Hamiltonian in the rotating wave approximation is:

$$V = -\frac{\hbar}{2}(\Omega_b|b\rangle\langle a| + \Omega_b^*|a\rangle\langle b| + \Omega_c|c\rangle\langle b| + \Omega_c^*|b\rangle\langle c|) \quad (1)$$

wherein Ω_b and Ω_c are Rabi frequencies corresponding to the (a) to (b) transition and to the (b) to (c) transition, respectively. Solving the equations of motion $\frac{\partial}{\partial t}|\phi(t)\rangle = -\frac{i}{\hbar}V|\phi(t)\rangle$ for a system initially in state $|\phi(0)\rangle = |a\rangle$ yields the state vector at time t (adapted from [57]):

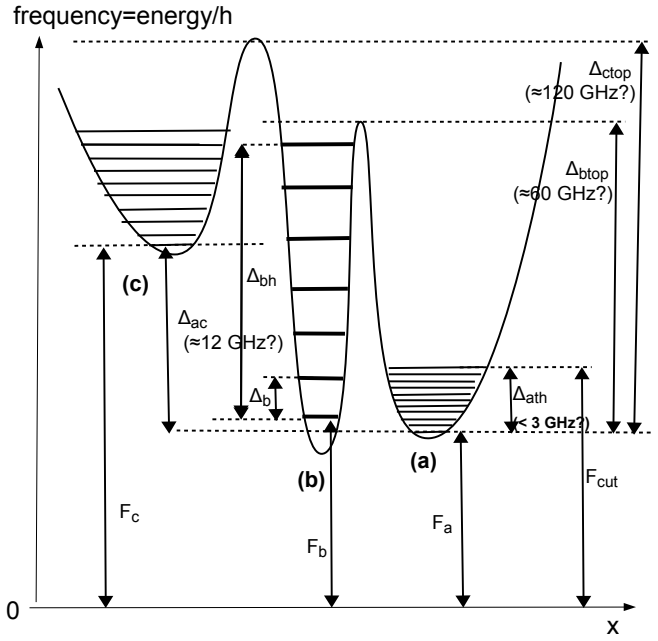

Figure 2: complete frequency/energy profile model. On this figure, the frequency of a quantum state is its energy divided by Planck's constant, so that the frequency difference between quantum states is the frequency of the transition. Horizontal bars in each well represent quantum states. Numerical values of frequency differences are reasonable values in view of the theory and experimental data. F_a [resp. F_b, F_c]: frequency of the fundamental state in well (a) [resp.(b)(c)]. Δ_b: frequency difference between adjacent quantum states in well (b). Δ_{ath}: frequency difference between the highest and lowest occupied energy states in well (a). Δ_{bh}: frequency difference between highest and lowest quantum states in well (b).

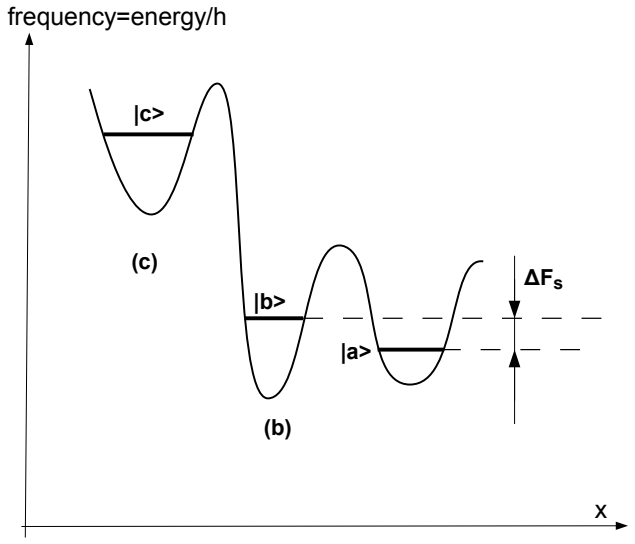

Figure 3: simplified energy profile model.

$$|\phi(t)\rangle = \left[\frac{\Omega_c^2}{\Omega_b^2+\Omega_c^2} + \frac{\Omega_b^2}{\Omega_b^2+\Omega_c^2}\cos\left(\frac{t}{2}\sqrt{\Omega_b^2+\Omega_c^2}\right)\right]|a\rangle + i\frac{\Omega_b}{\sqrt{\Omega_b^2+\Omega_c^2}}\sin\left(\frac{t}{2}\sqrt{\Omega_b^2+\Omega_c^2}\right)|b\rangle - \frac{\Omega_c\Omega_b}{\Omega_b^2+\Omega_c^2}\left[1-\cos\left(\frac{t}{2}\sqrt{\Omega_b^2+\Omega_c^2}\right)\right]|c\rangle \quad (2)$$

In particular:

$$|\langle c|\phi(t)\rangle|^2 = \left|\frac{\Omega_c\Omega_b}{\Omega_b^2+\Omega_c^2}\right|^2\left[1-\cos\left(\frac{t}{2}\sqrt{\Omega_b^2+\Omega_c^2}\right)\right]^2 \quad (3)$$

The probability of a transition of the TCR-pMHC from quantum well (a) to quantum well (c) after a suitable time is thus proportional to :

$$W_{trans} = \left|\frac{\Omega_c\Omega_b}{\Omega_b^2+\Omega_c^2}\right|^2 \quad (4)$$

In this "recognition" model I assume that $\Omega_c << \Omega_b$ so that equation 4 can be written:

$$W_{trans} \simeq \left|\frac{\Omega_c}{\Omega_b}\right|^2 \quad (5)$$

and I also assume that when the antigen p is the cognate antigen of the TCR, the value of Ω_b is minimized, yielding an increased probability of transition from well (a) to well (c), which characterizes recognition of the antigen.

2.2.2 The inhibitory effect (INH)

Pursuant to equation 5, when Ω_b increases, the probability W_{trans} diminishes. The Rabi frequency Ω_b being proportional to the electric field, if an artificial electromagnetic wave is present at the frequency corresponding to the $|a\rangle$ to $|b\rangle$ transition, then this electromagnetic wave will result in a diminished probability of the TCR-pMHC system reaching quantum well (c), i.e. in an inhibition (INH) of the recognition of the pMHC by the TCR.

The simple three-state configuration of figure 3 is thus sufficient to qualitatively understand how an artificial electromagnetic wave may inhibit the TCR-pMHC recognition. In this simple three-state configuration a significant inhibitory effect appears if the artificial wave has a frequency component on the frequency ΔF_s of the $|a\rangle$ to $|b\rangle$ transition, and has a power density (or irradiance) high enough to significantly modify Ω_b.

In the configuration of figure 2 the conditions for an inhibitory effect are as follows (see figure 2 for a definition of parameters F_a, F_b, Δ_{btop}, Δ_{ath}):

(i) bandwidth condition: Figure 4 shows quantum transitions between wells (a) and (c) and the range of an artificial electromagnetic wave, including its minimum frequency F_{min}, maximum frequency F_{max} and bandwidth Δ_{art}. On this figure the artificial electromagnetic wave can cause transitions from the quantum state $|a,0\rangle$ in well (a) to the quantum state $|b,0\rangle$ in well (b) but not to $|b,1\rangle$ or $|b,2\rangle$, and it cannot cause any transitions from

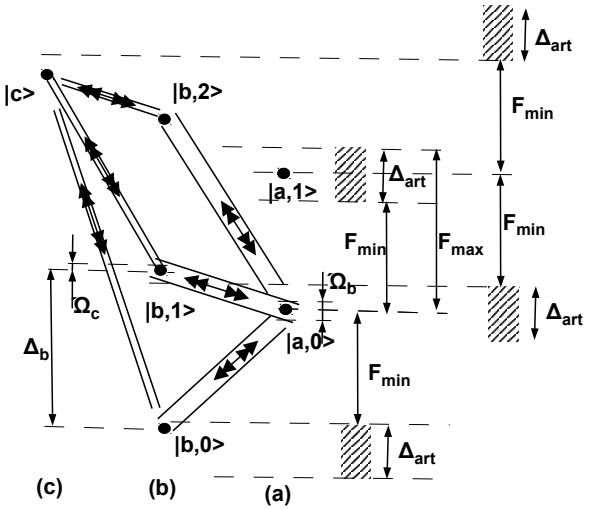

Figure 4: quantum transitions between quantum wells (a) (b) and (c). Each quantum state in each well is shown as a black dot. Δ_{art}: bandwidth of the artificial wave. F_{min}: minimum frequency of the artificial wave. F_{max}: maximum frequency of the artificial wave. Ω_b: Rabi frequency of the (a) to (b) transitions. Ω_c: Rabi frequency of the (b) to (c) transitions.

quantum state $|a,1\rangle$ to a quantum state in well (b). Essentially a quantum state in well (a) having a frequency $F_a + f$ can make transitions to any quantum state in well (b) which has a frequency between $F_a + f + F_{min}$ and $F_a + f + F_{min} + \Delta_{art}$, or between $F_a + f - F_{min}$ and $F_a + f - F_{min} - \Delta_{art}$. Both intervals have a width Δ_{art} so that generally, if $\Delta_{art} < \Delta_b$, there will be quantum states in well (a) that cannot make any transition to well (b) caused by the artificial electromagnetic wave. These quantum states of well (a) are basically un-influenced by the artificial electromagnetic wave and transitions from these states to well (c) occur as if the artificial electromagnetic wave was not present. Whenever any quantum states remain in well (a) which are un-influenced by the artificial electromagnetic wave, the inhibition of the (a) to (c) transition by the artificial electromagnetic wave is not limited by the Rabi frequency Ω_{bart} of the (a) to (b) transitions in the presence of the artificial wave, but rather by the proportion of quantum states in well (a) that are unaffected by the artificial wave and thus continue to have non-inhibited transitions to well (c). Therefore, the inhibition effect essentially has a bandwidth threshold. When $\Delta_{art} < \Delta_b$ this inhibition effect is very limited. When $\Delta_{art} > \Delta_b$ the inhibition effect can be much stronger as it is limited only by the power density of the artificial wave.

The above bandwidth dependency is somewhat mitigated by the fact that the effective bandwidth Δ_{art} is increased by twice the Rabi frequency $\frac{\Omega_{bart}}{2\pi}$ of the (a) to (b) transitions in the presence of the artificial wave. In particular, a continuous wave has a effective bandwidth $\frac{\Omega_{bart}}{\pi}$ which is non-zero, proportional to the electric field, and which for strong fields may allow a significant inhibitory effect despite the lack of bandwidth. This effective bandwidth is the range of frequencies contributing to stimulated emission/absorption as discussed in Appendix B.1 with a factor 2π due to the fact that Rabi frequencies are customarily expressed as angular frequencies. These considerations yield to a bandwidth condition which can be more fully expressed as:

$$\Delta_{art} + \frac{\Omega_{bart}}{\pi} > \Delta_b \tag{6}$$

However, even if this increased effective bandwidth in certain cases is sufficient to cause significant inhibition of the TCR-pMHC interaction by a single-frequency wave, this is expected to occur for a power density threshold way higher than the inhibition by an electromagnetic wave having the appropriate bandwidth $\Delta_{art} > \Delta_b$

(ii) Frequency condition: I consider a state $|a\rangle$ in quantum well (a) having a frequency $F_a + f$ with $F_b - F_a - f > 0$. Frequency shifts between $|a\rangle$ and other states in well (b) are all higher than $F_b - F_a - f$. Therefore, for the state $|a\rangle$ to be able to make a transition to any state of well (b), the artificial electromagnetic wave must comprise frequencies higher than $F_b - F_a - f$. This implies the condition $F_{max} > F_b - F_a - f$ where F_{max} is the maximum frequency of the artificial wave.

$F_b - F_a - f + \Delta_{btop}$ is is the frequency shift between state $|a\rangle$ and the maximum energy state of well (b). Frequency shifts between $|a\rangle$ and other states in well (b) are all lower than $F_b - F_a - f + \Delta_{btop}$. Therefore, for the state $|a\rangle$ to be able to make a transition to any state of well (b), the artificial electromagnetic wave must comprise frequencies lower than $F_b - F_a - f + \Delta_{btop}$. This implies the condition $F_{min} < F_b - F_a - f + \Delta_{bop}$.

Similar reasoning for the case $F_b - F_a - f < 0$ yields $F_{max} > -(F_b - F_a - f)$ and $F_{min} < -(F_b - F_a - f) + \Delta_{btop}$ so the conditions can be generally expressed as:

$$F_{min} - \Delta_{btop} < |F_b - F_a - f| < F_{max} \tag{7}$$

Since this condition must be verified by each f within the interval $[0, \Delta_{ath}]$ it results that the following frequency conditions must be respected:

$$F_{min} < \Delta_{btop} + \min_{0 \le f \le \Delta_{ath}} |F_b - F_a - f| \tag{8}$$

$$F_{max} > \max_{0 \le f \le \Delta_{ath}} |F_b - F_a - f| \tag{9}$$

As is the case for the bandwidth condition of equation 6 these equations are altered to take into account the supplementary bandwidth $\frac{1}{\pi}\Omega_{bart}$, yielding:

$$F_{min} - \frac{1}{2\pi}\Omega_{bart} < \Delta_{btop} + \min_{0 \le f \le \Delta_{ath}} |F_b - F_a - f| \tag{10}$$

$$F_{max} + \frac{1}{2\pi}\Omega_{bart} > \max_{0 \le f \le \Delta_{ath}} |F_b - F_a - f| \tag{11}$$

(iii) power condition An artificial wave which is a gaussian noise having its frequencies and bandwidth adapted to influence all (a) to (b) transitions is expected to have a significant inhibitory effect if its spectral power density (or spectral irradiance) is superior to the thermal

spectral power density at the same frequencies as given by Planck's equation. For example if $\Delta_{bth} = \Delta_{ath}$ and $F_a = F_b$ this artificial wave has frequencies between 0 and $\Delta_{art} = \Delta_{ath}$. Integration of the simplified Planck's equation equation 31 between 0 and Δ_{ath} yields the following integrated power density:

$$P = \frac{2\pi}{3}\frac{kT}{c^2}\left(\Delta_{ath}^3\right) \tag{12}$$

For example, for $\Delta_{ath} = \Delta_{bth} = 3$GHz this yields an integrated thermal power density $P = 8 \cdot 10^{-9}$ W/m2 corresponding to the power density threshold for an artificial wave having a 3 GHz bandwidth. Different configurations of the TCR-pMHC and of the artificial wave yield different thresholds. At least theoretically, any wave which has a spectral power density higher than the thermal spectral power density can cause a significant effect for a specific TCR-pMHC system having a corresponding configuration.

In short: a significant inhibitory effect will generally require at least the following conditions to be fulfilled:

(i) a bandwidth condition given by equation 6.

(ii) a frequency condition given by equations 10 and 11.

(iii) a power condition which depends on the bandwidth and frequency of the artificial wave and on the detailed configuration of the quantum wells.

2.2.3 Negative selection in the thymus (ENS)

As discussed in section 2.1 during negative selection the same TCR-pMHC recognition takes place which will also take place during the lifetime of a mature T cell, except that the recognition of an antigen (i.e. entry into quantum well (c)) triggers destruction of the T cell, rather than destruction of the APC. Thus, the inhibition of antigen recognition by an artificial electromagnetic wave also applies during the negative selection process. During the negative selection process, inhibition of antigen recognition can prevent elimination by negative selection (ENS) of a T cell which would not normally (i.e. absent the artificial wave) survive positive selection. This mechanism deeply modifies the overall effect of electromagnetic waves on the immune system. I will consider various cases:

- Effect on cancer after a low to high exposure transition: After a low to high exposure transition, the capacity of T cells to recognize cancerous cells is diminished. But T cells newly produced by the thymus after the transition are selected in high exposure conditions and will thus have a normal capacity to recognize the self in high exposure conditions. These newly produced T cells will also have a normal capacity to recognize cancerous cells, because cancerous cells are little different from normal "self" cells. After a certain time newly selected T cells will dominate and a normal behaviour of the immune system relative to cancer will be reinstated. The pro-cancer effect of a low to high exposure transition is thus temporary.

- Effect on cancer of temporary high exposure or alternating high/low exposure: Due to the inhibition of the TCR-pMHC recognition, selection steps that occur in the thymus in high exposure conditions fail to eliminate T cells which would be eliminated in low exposure conditions. When low exposure conditions are re-instated, these T cells become abnormally aggressive towards the self, resulting in an anti-cancer effect.

- Effects on infectious diseases after a low to high exposure transition: After a low to high exposure transition, ongoing immune responses against pathogens are weakened, which may result in a loss of control of the pathogen by the immune system. After a certain time a new primary immune response may yield to a new immune response able to control the pathogen. However, antigens of pathogens which do not mimic the self are clearly different from self antigens. Thymus selection reinstates a normal behaviour of the immune system towards self antigens but is unlikely to reinstate a normal behaviour of the immune system towards non-self antigens. Therefore a normal behaviour of the immune system towards infectious disease is not reinstated by thymus selection, and it is expected that there will be a long term pro-pathogen effect in high exposure conditions.

- Effects on infectious diseases of temporary or alternating high/low exposures: during high exposure periods there is a pro-pathogen effect but there is no appreciable modification of thymus selection with respect to non-self. Therefore during the low exposure periods the behaviour of the immune system relative to pathogens is essentially normal. The overall effect is pro-pathogen. If the high exposure periods represent a small fraction of the time, this pro-pathogen effect may however be negligible.

Auto-immune diseases, characterized by an excessive immune response against the self, are expected to react opposite to cancer, which is favoured by an insufficient immune response against self-like cancerous cells. Inflammatory diseases like pneumoconiosis, which are characterized by an excessive immune response against non-self, are expected to react opposite to infectious diseases, which are favoured by an insufficient immune response against non-self. These considerations are summarized in Table "INH+ENS" of Figure 8. However the results shown in this table must be considered jointly with the considerations described in sections 2.6.5 and 2.4, which limits its applicability "stricto sensu" to ideal conditions of low power density, high bandwidth, and thermal spectral power density as "low exposure" reference. Yet the table gives an efficient guideline for understanding many practical cases which may not be strictly ideal conditions.

2.2.4 The immuno-stimulatory effect (ST)

In equation 3 under the same conditions $\Omega_c << \Omega_b$ an increase of the Rabi frequency Ω_c is expected to result in an increase of $|\langle c|\phi(t)\rangle|^2$ corresponding to an stimulatory effect (ST) on the TCR-pMHC recognition. This immuno-stimulatory effect can be obtained by using an artificial electromagnetic wave having an appropriate frequency to cause transitions between wells (b) and (c), i.e. a frequency above roughly 9 GHz in the conditions of figure 2. As previously, a large bandwidth is expected to be more efficient than a low bandwidth. However, this is mitigated by the following facts:

If the artificial wave has a small bandwidth smaller than Δ_b or Δ_c, it may leave a number of states in well (b) or (c) un-affected. This slows down the transitions from (a) to

(c) however these transitions proceed through the affected states in (b) and (c) and therefore the (a) to (c) transition is slown down only in a proportionate manner as compared to the case of a large-bandwidth artificial wave. Importantly, it can be stimulated with arbitrary strength by using a sufficient power density. Thus, the threshold effect discussed in the case of the inhibitory effect (INH) of section 2.2.2 does not exist for the immuno-stimulatory effect (ST). The comparison between the (INH) and (ST) effects with regards to bandwidth can be summarized as follows: it is not possible to inhibit (a) to (c) transitions with arbitrary strength unless all pathes are simultaneously inhibited, but it is possible to stimulate (a) to (c) transitions with arbitrary strength by sufficiently stimulating a single path. Thus, even a low power density cw wave is expected to have some degree of efficacy in causing an immuno-stimulatory effect.

The probability of a transition from a state $|a,0\rangle$ in well (a) to a state $|c,0\rangle$ is well (c) is $\left|\frac{\Omega_c\Omega_b}{\Omega_b^2+\Omega_c^2}\right|^2$. If the artificial wave is strong enough to reverse the $\Omega_c << \Omega_b$ condition and yield $\Omega_c >> \Omega_b$ then the likelihood of this transition is again extremely low. Therefore, high-power strictly cw waves cannot cause significant transitions.

This stimulatory (ST) effect on the TCR-pMHC recognition is expected to also affect negative selection in the thymus, in a manner opposite to the inhibitory effect (INH). For permanent exposures or for transitions, this yields effects opposite to those of Table "INH+ENS" columns A to D on Figure 8. For temporary exposures lasting shortly, for example 1 h/day, during exposure some T cells are eliminated by negative selection which would normally have survived negative selection. This results - prima facie - in a pro-cancer effect opposite to that of Table "INH+ENS". However, the number of eliminated T cells is only a small part of thymus production. Recognition of neoplasms can proceed through non-eliminated T cells which are a majority. The effect of thymus selection on tumour regression is thus negligible. However, during exposure periods the otherwise normal T cells become abnormally aggressive. This abnormal aggressiveness results in increased anti-cancer efficiency even if it applies only part-time: 1 hour per day of systematic tumour cell elimination is more efficient than 24 hour/day of un-ability of T cells to attack tumour cells. Therefore in the case of short temporary exposures as per Table "INH+ENS" column E, the effects on diseases of the stimulatory (ST) effect is anti-cancer.

The comparison of the effects on cancer of repeated short exposures for effects (ST) and (INH) can be summarized as follows: one abnormally aggressive T cell can be sufficient to overcome a cancer, so in (INH) a few abnormally aggressive cells produced by the thymus can yield a significant anti-cancer effect. But a few under-aggressive T cells do not notably degrade anti-cancer efficiency, so in (ST) the stimulatory, anti-cancer effect directly resulting from exposure dominates over the pro-cancer effect resulting from modified thymus selection. However, if after one or a few exposure periods there is a long-lasting non-exposure, the pro-cancer effect may dominate during the long-lasting non-exposure because during the long-lasting non-exposure there is no direct effect, so the only remaining effect is due to thymus selection prior to the long-lasting non-exposure period.

Thus, the consequences of this immuno-stimulatory effect on diseases are essentially opposite to the predictions of "INH+ENS" except that for column E in the case of repeated exposures the effect is anti-cancer for reasonably short exposures and until the end of the repeated exposures. These effects are summarized in Table "ST+ENS" on Figure 8.

2.2.5 Stimulatory effects of a high-power amplitude-modulated cw wave (STM)

When the initial quantum state of the system is $|b\rangle$ instead of $|a\rangle$ then equation 2 is replaced by:

$$\begin{aligned}|\phi(t)\rangle = &\cos\left(\frac{t}{2}\sqrt{\Omega_b^2+\Omega_c^2}\right)|b\rangle \\ &- i\frac{\Omega_b}{\sqrt{\Omega_b^2+\Omega_c^2}}\sin\left(\frac{t}{2}\sqrt{\Omega_b^2+\Omega_c^2}\right)|a\rangle \\ &- i\frac{\Omega_c}{\sqrt{\Omega_b^2+\Omega_c^2}}\sin\left(\frac{t}{2}\sqrt{\Omega_b^2+\Omega_c^2}\right)|c\rangle \quad (13)\end{aligned}$$

If the cw wave is strong enough to yield $\Omega_c >> \Omega_b$ (which will be assumed throughout this section) then equation 13 yields:

$$|\phi(t)\rangle = \cos\left(\frac{t}{2}\Omega_c\right)|b\rangle - i\sin\left(\frac{t}{2}\Omega_c\right)|c\rangle \quad (14)$$

Assuming the initial state is $|b\rangle$ and a pulsed wave stimulates the (b) to (c) transition, with a pulse length T and a value $\Omega_c = \Omega_{cart} >> \Omega_b$ for the duration of the pulse:

- if $\frac{T}{2}\Omega_{cart} = 2\pi k$, k an integer, then at the end of the pulse the system is back to state (b).

- if $\frac{T}{2}\Omega_{cart} = \pi + 2\pi k$, k an integer, then at the end of the pulse the system is in state (c).

So depending on pulse length and power density, a pulse can either be neutral (i.e. leave the system in its original well (b)) or transfer quantum state $|b\rangle$ to quantum state $|c\rangle$. In the absence of any artificial wave, the transitions are ruled by equation 2 and since $\Omega_c << \Omega_b$ the quantum state essentially alternates between quantum wells (a) and (b) with a very low transition rate to well (c). When the pulse starts, the quantum state may thus be either $|a\rangle$ or $b\rangle$, with essentially a probability of $\frac{1}{2}$ for each. If it is in state $|b\rangle$ then the pulse, if it has an appropriate duration and power density, will transfer it to well (c).

Therefore, the effect of a pulse will either be neutral or stimulatory, dependent of its power density and duration. The presence of a plurality of quantum states in each quantum well is expected to yield less efficient transitions (because not every quantum state is directly affected by the pulse) but the above reasoning still gives at least a qualitative understanding of the dependency on pulse length and power density.

If the wave is a cw wave sinusoidally modulated with a frequency f_{mod} then in first approximation it may be considered as a series of pulses having duration $T = \frac{1}{2f_{mod}}$ which for sufficiently high value of f_{mod}, as discussed in

the previous paragraph, can cause either stimulatory or inhibitory effects. The Rabi frequency during the pulse is $\Omega_{cart} = C\sqrt{P_{art}}$ wherein C is a coefficient independent of the power density of the artificial wave and P_{art} is the power density of the artificial wave. The condition for a maximum [resp. minimum] transfer to well (c) and thus maximum [resp.minimum] immuno-stimulatory effect is:

$C\frac{\sqrt{P_{art}}}{2f_{mod}} = \epsilon\pi + 2\pi k$

with k an integer, and $\epsilon = 1$ [resp. $\epsilon = 0$] for the maximum [resp.minimum] immuno-stimulatory effect.

At a constant power density P_{art} the immuno-stimulatory effect is maximized [resp.minimized] for the following values of modulation frequency of the modulated artificial wave:

$$f_k = C\frac{\sqrt{P_{art}}}{2\pi(\epsilon + 2k)} \tag{15}$$

Thus, alternating maximums of the stimulatory effect dependent on the frequency of the amplitude modulation are expected to be observable when the artificial wave is in the frequency range that stimulates the (b) to (c) transitions. The expected effects of these alternating maximums are represented as "STM+ENS" in Figure 8. Positions of these minimums and maximums are given - ignoring the presence of multiple quantum states in each quantum well - by equation 15. Likewise, if frequency is kept constant, power density-dependent peaks are expected.

2.3 Fever and hyperthermia theory (FEV)

In this section i develop a theory of fever and hyperthermia which is essentially based on the recognition mechanism (RE).

2.3.1 normal conditions

I now assume that potential well (a) is in contact with a thermostat. Also assuming that the degree of liberty x of figure 2 is independent of other degrees of liberty, the statistical distribution of energy states E_i in quantum well (a) along degree of liberty x follows approximately the distribution $P_i = \frac{1}{Z}e^{-\frac{E_i}{kT}}$ wherein E_i is the energy in quantum state number i and P_i is the probability of occupation of quantum state number i. Following the conventions of figure 2 i use an absolute frequency $F_i = \frac{E_i}{h}$ to characterize each quantum state, so that the frequencies corresponding to transitions can be calculated as differences between absolute frequencies. The distribution is then written $P_i = \frac{1}{Z}e^{-\frac{hF_i}{kT}}$. In a first degree approximation this probability varies linearly and cancels at absolute frequency $F_{canc} = \frac{kT}{h}$. In well (a) the probability of occupation of a quantum state is cut by half between frequency F_a and frequency $F_{cut} = F_a + \frac{1}{2}(F_{canc} - F_a)$. In the simplified picture of constant occupation probabilities in well (a) i can thus take the maximum frequency of occupied levels to be equal to $F_{cut} = \frac{kT}{2h} + \frac{1}{2}F_a$.

When temperature rises by ΔT the frequency F_{cut} rises by $\Delta F_{cut} = \frac{k\Delta T}{2h}$. Normal diurnal temperature variations are between 0.5 and 1 degree corresponding to a variation ΔF_{cut} of 5 to 10 GHz. These variations are reasonably consistent with the hypothesis that the occupied levels of well (a) would essentially remain below the fundamental levels of well (c) corresponding to absolute frequency F_c on figure 2. Further, the interaction between well (a) and the thermostat may be weak, so that the temperature variations do not instantaneously reflect in variations of the occupied levels of well (a). In such case, the changes in occupied levels in well (a) can be viewed as reflecting a time-filtered version of temperature changes, so that the variation of ΔF_{cut} is below the 5 to 10 GHz figure. Thus, the (lower) frequencies which promote (a) to (b) transitions and have an inhibitory effect on the TCR-pMHC recognition remain essentially distinct from the (higher) frequencies which promote (b) to (c) transitions and have a stimulating effect on the TCR-pMHC recognition. Qualitatively, at all times artificial waves below 3 GHz are expected to affect essentially the (a) to (b) transitions so that their health consequences remain as shown in Table "INH+ENS" of Figure 8.

2.3.2 fever or mild hyperthermia

The overlap between wave functions in adjacent wells (a) and (b) (or (c) and (b)) is generally expected to increase as the energy of the wave functions gets nearer to the top of the quantum barrier separating wells, because when it passes the top of the energy barrier the wave functions the system may classically move between the wells, which roughly corresponds to a maximum value of the overlap (in this case eigenfunctions are not restricted to either well but the overlap between wave functions which are restricted to either quantum well and are not eigenfunctions can still be calculated and be near 1). The Rabi frequency of a transition between adjacent wells is proportional to the overlap (see Appendix A) and is thus also expected to increase. However when the energy of the quantum states gets very near to the top of the barrier, the overlap which cannot become larger than 1 increases more slowly and the Rabi frequency also increases more slowly.

Thicker or higher barriers between quantum wells yield smaller overlaps and thus lower Rabi frequencies. Thus the condition $\Omega_c << \Omega_b$ implies that the barrier between (a) and (b) is lower/thinner than the barrier between (b) and (c) as shown on Figure 2.

In case of fever (FEV), temperature rises by about 3 degrees. This rise yields an increase of F_{cut} which is about 30 GHz, coming clearly above the fundamental level F_c in well (c). When F_{cut} increases both Ω_b and Ω_c increase but since the energy in well (b) is nearer to the top of the corresponding energy barrier, the corresponding Rabi frequency Ω_b is expected to increase more slowly. Therefore the value $\max(|\langle c|\phi(t)\rangle|^2) = 2\left|\frac{\Omega_c\Omega_b}{\Omega_b^2+\Omega_c^2}\right|^2 \simeq 2\frac{\Omega_c}{\Omega_b}$ increases, corresponding to a stimulatory effect on the TCR-pMHC recognition. The expected effect on cancer is influenced by thymus selection: the short term effect is anti-cancer and the long term effect is pro-cancer due to the excessive elimination of T cells by negative selection in the thymus during hyperthermia and possibly because some T cells which escape positive selection during hyperthermia may slow down access to the tumor. The pro- and anti-cancer effects compete with each other to yield an overall effect on

a specific tumor started at a specific point in time relative to the hyperthermia sessions.

2.3.3 strong hyperthermia

If temperature is further increased up to 43 degrees, corresponding to an increase of F_{cut} which is roughly 60 GHz above F_a, the energy of the quantum states in wells (a) and (b) becomes higher that the barrier between the wells. The two wells tend to act as a single well. The interaction in a simplified model can be modeled as an interaction between well (a') corresponding to (a) and (b) re-united, and well (c), with a Rabi frequency Ω_c which is presumably low pursuant to the hypothesis $\Omega_c << \Omega_b$.

In this interaction, equation 3 is replaced by (adapted from [57]):

$$|\langle c|\phi(t)\rangle|^2 = \sin^2\left(\frac{\Omega_c t}{2}\right) \tag{16}$$

Whilst in equation 3 the oscillation frequency was $\frac{1}{2}\sqrt{\Omega_b^2+\Omega_c^2} \simeq \frac{\Omega_b}{2}$ in equation 16 the oscillation frequency is $\frac{\Omega_c}{2} << \frac{\Omega_b}{2}$. This very low oscillation frequency may be the limitating condition, yielding to an inhibition of the TCR-pMHC recognition.

2.4 Interaction mechanism for non-recognition of abnormal antigens by T cells (NRE)

2.4.1 The "non-recognition" mechanism (NRE)

The "non-recognition" model is based on transitions between quantum wells (a'), (b'), (c') which may or may not be partially the same like quantum wells (a) , (b), (c) but which are at least assumed to have essentially the same configuration as wells (a), (b), (c) as shown of figure 2. One hypothesis is that wells (a) and (a') [resp. (b) and (b')] are the same, whilst wells (c) and (c') are different; however there is some uncertainty on this issue so (a') and (b') will not generally be assumed to be the same as (a) and (b) respectively. The Rabi frequency of the transition from (a') to (b') is $\Omega_{b'}$ and the Rabi frequency of the transition from (b') to (c') is $\Omega_{c'}$. However, the hypothesis on $\Omega_b >> \Omega_c$ is replaced by $\Omega_{b'} << \Omega_{c'}$. The probability of reaching well (c') is given by equation 4 wherein (a,b,c) are replaced by (a',b',c'). Since $\Omega_{b'} << \Omega_{c'}$, equation 4 yields:

$$W_{trans} \simeq \left|\frac{\Omega_{b'}}{\Omega_{c'}}\right|^2 \tag{17}$$

When $\Omega_{b'}$ decreases the probability of transfer to well (c') decreases, and vice versa. Transfer from well (a') to well (c') is thus favoured by non-recognition of the antigen, rather than recognition of the antigen. It is further hypothesized that from well (c') the system evolves predictably to the Temporarily Inactivated (TI) state discussed in section 2.1, in which it remains unable to recognize antigens for a certain time.

2.4.2 Positive selection in the thymus (EPS)

As discussed in section 2.1, it is assumed in the present model that the Non-Recognition mechanism is based on the same mechanism during positive selection as during temporary inactivation, except that reaching quantum state (c') triggers Elimination of the T cell by Positive Selection (EPS) instead of its temporary inactivation (TI).

2.4.3 sensitivity to artificial waves affecting $\Omega_{b'}$ (INA)

Application of an electromagnetic wave (typically below 3 GHz) increasing the $\Omega_{b'}$ in a "non-recognition" (NRE) mechanism ruling recognition of self antigens can cause non-recognition of the self antigen and temporary inactivation (INA) of the T cell.

In the "non-recognition" mechanism, if the artificial wave is single-frequency (cw), it may leave a number of states in well (a) un-affected. But thermal exchanges between these states may "re-fill" the affected quantum states from the non-affected ones in a time scale significantly shorter than the interaction time, so that the entirety of the probability of presence may progressively shift from quantum well (a) to quantum well (c) over the duration of the interaction. Thus, even a low power density cw wave is expected to have some degree of efficacy in causing an immuno-stimulatory effect. This effect is expected to be increased if the bandwidth is increased, but the extent of such increase is dependent upon thermal relaxation effects which are not properly known.

The lesser importance of bandwidth differs from the case of the "recognition" mechanism because if an artificial wave intended to cause an inhibitory effect in the "recognition" mechanism leaves any quantum states in (a) non-affected, the probability of presence will shift from these quantum states to quantum state (c) in a non-reversible manner, substantially cancelling any inhibitory effect on other quantum states. The fundamental difference is that in one case the single-frequency artificial wave triggers a modest but non-reversible effect which can build up over time, whilst in the other case it causes a modest inhibition whilst the dominant transitions remain in place and the non-reversible effect is caused by these dominant transitions. The difference between the temporary inactivation by an artificial wave (INA, based on the non-recognition mechanism NRE) and the temporary inhibition by an artificial wave (INH, based on the recognition mechanism RE) in this respect is similar to the difference between inhibition (INH) and stimulation (ST).

Due to the higher sensitivity of temporary inactivation (INA) to single frequency waves, the temporary inactivation effect (INA) of single-frequency electromagnetic waves pursuant to the non-recognition (NRE) mechanism is expected to dominate over the inhibitory effect (INH) pursuant to the recognition mechanism (RE) for a range of power densities of a cw artificial wave. The two mechanisms may also be jointly affected in case high power density large bandwidth artificial waves are used.

2.4.4 Interaction of temporary inactivation with thymus selection

In the thymus, positive selection takes place before negative selection. Absent any artificial wave, positive selection eliminates any T cells that would become inactivated following an interaction with self antigens. Therefore when after transit through the "positive selection" part of the thymus, surviving T-cells reach the "negative selection" part of the thymus, they are not normally "temporarily inactivated" upon any encounter with self antigens, so that they can undergo the whole positive selection without being temporarily inactivated.

In case of exposure to an artificial wave affecting $\Omega_{b'}$, if the power density of the artificial wave is strong enough and if exposure is permanent or is repeated often enough, substantially all T cells are exposed at some point during transit through the "positive selection" part of the thymus and thus get eliminated by positive selection (EPS), yielding a pro-cancer effect and generally the effects summarized in Table "INA+EPS" in Figure 8. In particular, effects remain pro-cancer and pro-pathogen in the period immediately following a high to low exposure transition, because during high exposure thymus output is essentially stopped, which results in a long-lasting depletion of the numbers of T cells.

However if the power density of the artificial wave is relatively weak, or if exposure is rare, most T cells survive positive selection and some T cells survive positive selection steps in non-exposed conditions whilst they would not have survived the same steps in exposed conditions. These latter T cells may become temporarily inactivated (INA) during negative selection if they encounter in exposed conditions an antigen which they encountered in non-exposed conditions during positive selection. A T cell which is temporarily inactivated (INA) during negative selection escapes subsequent negative selection steps until it becomes re-activated, so that it may survive negative selection whilst it would not have survived normally (i.e. if it had not been temporarily inactivated). Such T cell after leaving the thymus is abnormally aggressive towards self antigens in non-exposed conditions (provided such non-exposed conditions last long enough for it to be re-activated) and thus causes an auto-immune effect. This effect is summarized in Column R of Table "INA+EPS+ENS" in Figure 8.

Thus, temporary inactivation "in vivo" (INA) can result either in an auto-immune effect (for low power density and/or rare exposures) or in a pro-cancer effect (for high power density frequent or permanent exposures).

2.4.5 sensitivity to artificial waves that affect $\Omega_{c'}$ (LIN).

An artificial wave that increases $\Omega_{c'}$ causes a decrease of the transition probability to well (c') and thus prevents the temporary inactivation of corresponding TCRs yielding a lack of inactivation (LIN). As this effect is in essence inhibitory it has a bandwidth condition similar to equation 6 but based on the frequency step between quantum states in well (c'):

$$\Delta_{art} + \frac{\Omega_{c'art}}{\pi} > \Delta_{c'} \tag{18}$$

wherein Δ_{art} is the bandwidth of the artificial wave, $\Delta_{c'}$ is the frequency step between states in well (c'), and $\Omega_{c'art}$ is the Rabi bandwidth of the (b') to (c') transition stimulated by the artificial wave.

This effect (LIN) is predicted by theory but has not been observed. The frequency of the corresponding artificial wave is unknown, but must be different than the frequencies causing temporary inactivation (INA), otherwise it would be impossible to increase $\Omega_{b'}$ without simultaneously increasing $\Omega_{c'}$, so that there would not be an observable temporary inactivation (INA) effect. It may therefore be typically above 9 GHz as represented in figure 2 for the recognition mechanism, but other configurations are not excluded.

2.5 A global view of the model.

The inter-relation between the recognition mechanism and the non-recognition mechanism is not known in detail. However the two mechanisms are not expected to be independent. The arrangement of the two mechanisms must be such that the T cell does not become temporarily inactivated when it encounters its cognate antigen, which could potentially happen if the mechanisms were fully independent. One possibility is that wells (a) and (a') [resp. (b) and (b')] are the same well, with (c) and (c') being different wells, as represented on figure 5. This yields $\Omega_b = \Omega_{b'}$, with entry into well (c) characterizing recognition (RE) and entry into well (c') characterizing non-recognition (NRE). This also guarantees that a T cell does not become temporarily inactivated when it encounters its cognate antigen.

Figures 6 and 7 are diagrams illustrating the present model. Reading these figures we can assume $\Omega_b = \Omega_{b'}$. Alternatively, the figures remain valid but the approach to the to the TI-EPS areas is ruled by the value of $\Omega_{b'}$ whilst the approach to the DES-ENS areas is ruled by the value of Ω_b. In the case of figure 7 the vertical axis can also be taken as representing the logarithm of the power density P_{bart} of the artificial wave in the 0-3 GHz range. Figures 6 and 7 show the value of $\log \Omega_c$ on the horizontal axis and the value of $\log \Omega_b$ and $\log \Omega_{b'}$ on the vertical axis.

It is assumed that under natural conditions a decrease of Ω_b characterizes recognition of an antigen, whether of the self or of the non-self. As shown on figure 6 the recognition of an antigen (RE) diminishes the value of Ω_b and brings the TCR-pMHC system towards an area DES-ENS corresponding to destruction of the APC (in the case of an effector T cell) or elimination of the T cell (in the thymus). The borders of the DES-ENS area correspond to a fixed value of $\frac{\Omega_b}{\Omega_c}$ and thus to a right line parallel to the $\Omega_b = \Omega_c$ line.

Similarly, non-recognition (NRE) corresponds to an increase of Ω_b as compared to its value in the Neutral Area and brings the TCR-pMHC system towards the area TI-EPS corresponding to temporary inactivation (in the case of an effector T cell) and elimination by positive selection (in the thymus).

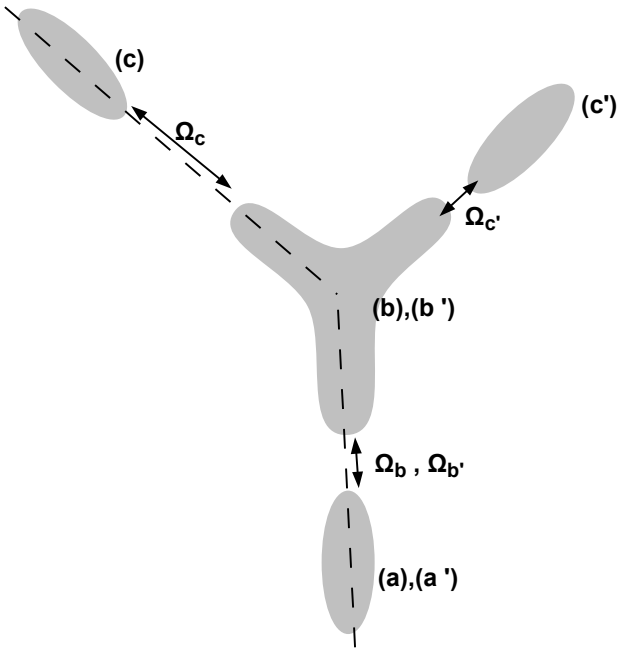

Figure 5: Example of an arrangement of quantum wells shown in a 2-dimensional space. Gray areas are low-energy areas corresponding to quantum wells. Figure 2 would then represent the energy profile along the minimum energy line shown (dotted line).

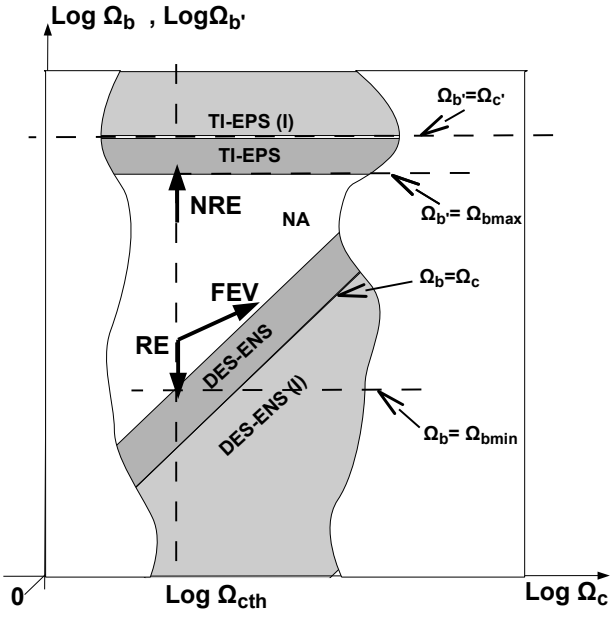

Figure 6: Functional diagram of the TCR-pMHC recognition mechanism showing Temporary Inactivation (TI) area, Elimination by Positive Selection (EPS) area, APC Destruction (DES) area, Elimination by Negative Selection (ENS) area, Neutral Area (NA). Arrows represent Recognition of an antigen (RE), non-recognition (NRE), fever (FEV). Areas labelled (I) are not normally reached. P_{bart} [resp. P_{cart}] is the power density of the artificial wave which affects Ω_b [resp. Ω_c].

Overall, for effector T cells, the whole mechanism results in the T cell destructing its target when the recognition is strong enough to bring the TCR-pMHC system in the DES-ENS area, and in the T cell being temporarily inactivated when it does not recognize any target (whether of the self or non-self). In-between, there is a neutral area in which the T-cell simply remains active, typically when it recognizes a self antigen. Because self-antigens are also presented in the thymus and T cells which on recognition of a self antigen reach the DES-ENS area are eliminated in the thymus by negative selection, effector T cells having survived negative selection do not normally enter the DES-ENS area on recognition of self antigens. Similarly, T cells which enter the TI-EPS area on recognition of a self antigen are eliminated in the thymus, and surviving effector T cells never enter the TI-EPS area on recognition of self antigens. But, a T cell (more precisely the corresponding TCR-pMHC systems) enters the DES-ENS area if it encounters its cognate (non-self) antigen, and it enters the TI-EPS area if it encounters a non-self antigen to which it is unable to bind.

In the case of fever or mild hyperthermia (FEV), as discussed in section 2.3, there is an increase of both Ω_c and Ω_b but the increase in Ω_c is stronger , yielding to the system possibly entering the DES-ENS area whilst it would not have done so at normal body temperatures.

Figure 7 shows, on the same two-dimensional diagram, the effect of various electromagnetic waves. A wave affecting Ω_b (INH) (typically in the 0-3 MHz range) yields an inhibitory effect on T cell recognition, because it can bring a TCR-pMHC system out of the DES-ENS area towards the neutral area. In the thymus, the fact that a T cell leaves the DES-ENS area means that it will survive thymus selection, which it would not have done otherwise. However, if the power density of the wave is too strong , the same or another T cell may enter the TI-EPS area (arrow INA). In this case, it will again be eliminated in the thymus, this time by positive selection.

Similarly a wave affecting Ω_c (typically in a frequency range higher than 9 GHz) will bring a TCR-pMHC system towards the DES-ENS area (arrow ST) yielding an increased tendency of the T cell to destruct the APC (in the case of an effector T cell). In the thymus, it can cause a T cell to be eliminated by positive selection, which would otherwise have survived. Thus the effects of this wave are opposite to the effects of a wave affecting Ω_b as discussed in section 2.2.4.

Cancers and auto-immune diseases are related to TCR-pMHC systems which are near the border of the DES-ENS region. For low power densities of an electromagnetic wave affecting Ω_b, it is clear that these TCR-pMHCs can move in and out of the DES-ENS region due to the INH effect, but they are unlikely to move to the TI-EPS region which is much farther on the diagram. Thus for low power density, high bandwidth electromagnetic waves affecting Ω_b, cancers and auto-immune diseases are expected to be affected by the (INH) effect, but not by the (INA) effect. However, infectious diseases and inflammatory diseases are related to T cells that can be anywhere in the neutral area, so that they may be affected both by the (INH) and (INA) effects even for low power density, high bandwidth waves.

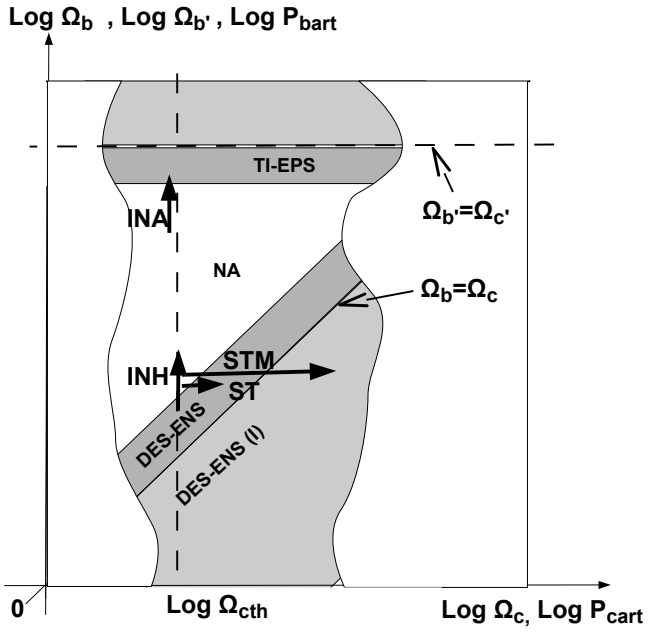

Figure 7: Effects of artificial electromagnetic waves on TCR-pMHC systems showing Temporary Inactivation (TI) area, Elimination by Positive Selection (EPS) area, APC Destruction (DES) area, Elimination by Negative Selection (ENS) area, Neutral Area (NR). Areas are labelled(I) when the normal ratio between Ω_b and Ω_c is inversed. Arrows represent Inhibition (INH, see section 2.2.2), Stimulation (ST, see section 2.2.4),Temporary Inactivation (INA, see section 2.4), strong Stimulation with modulation useful (STM, see section 2.2.4)

.

Figure 8 summarizes the mechanisms discussed in the previous sections, with indication of typical power densities, bandwidths of frequencies, in part deduced from experimental data which will be discussed in the next sections.

In Figure 8: Typical power densities are deduced from experimental data. Frequencies between 3 and 9 MHz are not shown because there is no experimental data. Likewise, some intermediate power density ranges in which there is no data are not shown. *: A,B,C,D,E as defined in Table "INH+ENS". wb: wideband. cw:continuous wave. lb: low bandwidth, but a minimum bandwidth in the order of a few 100 Hz may be necessary, see section 3.1.2. (a): pathogens that do not mimic the self. (b) inflammatory diseases directed against non-self. Any inflammations directed against the self are considered auto-immune. (c) exposures frequent enough so that temporarily inactivated cells remain inactivated between exposures, for example daily exposures. A minimum duration of the individual exposure may also be necessary for this effect. (d): rare means sufficiently rare so that any temporarily inactivated cells are re-activated at least half of the time. (e): strongest auto-immune effect at this power density regime, period of alternative exposures allows inactivated T cells to bypass negative selection, following non-exposure period re-activates these T cells yielding auto-immune effect. (f): standard (normal aggressiveness of T cells) with respect to permanent low exposure, not with respect to the previous exposure. T cell count may be diminished. (g) no effect predicted by a simple theory, but inhibitory or inactivatory effect observed, see section 3.2.4. (h) a connection between anti-autoimmune effects and disturbances of developmental endpoints is established experimentally, see section 3.1.3.(i) see section 3.1.10 for an exception. (j) this case remains dominated by "INH+ENS". (k) depends on the reasoning in section 2.6.6.

2.6 Other aspects which may impact the model

2.6.1 Regulatory mechanisms

In [56] stimulation of mixed (i.e. not monoclonal) T cells by either autologous irradiated non-T cells or allogeneic non-T cells results in proliferation of the mixed T cells. The proliferation of the mixed T cells stimulated by autologous irradiated non-T cells is impaired in mixed T cells of elderly subjects as compared to adults between the ages of 20 and 32, but the proliferation of mixed T cells stimulated by allogeneic non-T cells is not impaired in mixed T cells from elderly subjects.

Antigens presented by autologous irradiated non-T cells are near-self so that they tend to be recognized by T cells which are more aggressive towards the self. Antigens presented by allogeneic non-T cells are not near self and can be recognized by T cells which are not particularly aggressive towards the self. The impaired proliferation in elderly

Mechanism	Natural outcome (effector T cells)	Natural outcome (in Thymus)	Condition	Direct Effect of Exposure	Change in Rabi freq.	Typ. wave freq.	Typical wave modulation
Recognition (RE)	Destruction of APC (DES)	Elimination by Negative Selection (ENS)	$\Omega_c << \Omega_b$	Inhibition (INH)	$\Omega_b \nearrow$	<3 GHz	wb
				Stimulation (ST)	$\Omega_c \nearrow$	>9 GHz	cw / wb
				Alternating (STM)	$\Omega_c \uparrow\uparrow$		(cw/wb) with am
				Stimulation(FEV) (Hyperthermia)	$\Omega_b \nearrow$ $\Omega_c \uparrow\uparrow$	-	
Non-Recognition (NRE)	Temporary Inactivation (TI)	Elimination by Positive Selection (EPS)	$\Omega_{c'} >> \Omega_{b'}$	Temporary inactivation (INA)	$\Omega_{b'} \nearrow$	<3 GHz	lb/wb
				Lack of inactivation (LIN)	$\Omega_{c'} \nearrow$	>9 GHz ?	wb

	A	B	C	D	E
Column description	Permanent low exposure (thermal)	Permanent high exposure	Transition from Low to High exposure: period immediately after transition	Transition from High to Low exposure : period immediately after transition	Alternance between low and high exposure (at least half time low exposure)

INH+ENS	A	B	C	D	E
cancer	standard	Standard(i)	Pro cancer	Anti cancer	Anti cancer
auto-immune disease	standard	standard	Anti-autoimmune	Pro-autoimmune	Pro-autoimmune
pathogen (a)	standard	Pro pathogen	Pro pathogen	standard (f)	Pro pathogen
inflammatory disease (b)	standard	Anti-inflammatory	Anti - inflammatory	standard (f)	Anti-inflammatory
Developmental timing	standard	standard	delayed ? (k)	Accelerated ? (k)	Accelerated ? (k)

wb, typ. power density <0.01 W/m2

lb/wb, typ. power density : >0.5 W/m2

INA+EPS+ENS	A	F: B, C, frequent exposures (c)	D(j)	R: rare short exposures (d) OR alternating exposures then non-exposure (e)
cancer	standard	Pro cancer		Anti cancer
auto-immune disease	standard	Anti-autoimmune		Pro-autoimmune
pathogen (a)	standard	Pro pathogen		standard(f)
inflammatory disease (b)	standard	Anti – inflammatory		standard(f)
developmental timing	standard	Disturbed (h)		accelerated ? (k)

Typ. power density< 10 W/m2

typ. power density>50 W/m2, typ. exposure time > 1h/day

INA+EPS	A	B,C,D,E (incl. cases (d) and (e))
cancer	standard	Pro cancer
auto-immune disease	standard	Anti-autoimmune
pathogen (a)	standard	Pro pathogen
inflammatory disease (b)	standard	Anti-inflammatory
Developmental timing	standard	Disturbed (h)

<3 GHz

>9 GHz

ST +ENS	A	B	C	D	E
cancer	standard	standard	Anti cancer	Pro cancer	Anti cancer
auto-immune disease	standard	standard	Pro-autoimmune	Anti-autoimmune	Pro-autoimmune
pathogen (a)	standard	Anti pathogen	Anti pathogen	standard (f)	Anti pathogen
inflammatory disease (b)	standard	Pro-inflammatory	Pro - inflammatory	standard (f)	Pro-inflammatory

Typ. power density <0.01 W/m2

Typ. power density > 300 W/m2

Power & frequency maximize stimulation

power & frequency dependent peaks of STM

Power & frequency Minimize stimulation

STM + ENS (max)	Same as ST+ENS	STM+ENS (min)	(?) (g)

Band-limited artificial waves

Thermal exposure

Short term effect of temporary whole-body hyperthermia (FEV+ENS)	Long term effect of temporary whole-body hyperthermia (FEV+ENS)	Short and long term effect of temporary Local hyperthermia (FEV only)
Anti-cancer	Pro-cancer	Anti-cancer

Figure 8: Mechanisms and effects. See box in text for details.

subjects for near-self antigens shows that these subjects have less of the more aggressive T cells, but the normal reaction of the same towards the allogeneic T cells shows that their other T cells have a normal capacity to recognize non-self antigens.

Thus, there exists a mechanism which results in a diminished proportion of T cells aggressive towards the self in elderly people. This mechanism is extra-thymic, because there is little thymic activity in the elderly. This mechanism is thus an extra-thymic regulatory system adapted to eliminate excessively aggressive T cells.

This extra-thymic regulation mechanism may work essentially in the same way as negative selection in the thymus, i.e. following an interaction based on the "recognition" mechanism the interacting T cell would be destructed instead of the APC being destructed. The regulation mechanism would thus be based on specialized APCs capable of destructing T cells. Such specialized APCs may include regulatory T cells. It is likely that each interaction yielding destruction of a T cell further stimulates the specialized APC into dividing more often, so that the growth of the number of abnormally aggressive T cells is met by a growth in the number of specialized APCs capable of destructing them. Therefore, the size and thus the efficiency of the regulation system as a whole evolves depending of how much it is solicited.

This regulatory mechanism participates in defining the time evolution of the immune response following a change in the radio-frequency environment.

In particular, pursuant to Table "INH+ENS" column E in figure 8, time-varying waves cause auto-immune effects. In such situations, a number of abnormally aggressive T cells are present outside the thymus. The extra-thymic regulation mechanisms can progressively eliminate these cells.

2.6.2 Inhibitory receptors

The theory which applies to the TCR-pMHC recognition may also, to some extent, apply to other cell receptors. Many T cells (sometimes called NK T cells, and not to be confused with NK cells, which lack TCRs) have inhibitory receptors that participate in the regulation of the immune response ([42], [37], [1], [36]). These receptors do quantitatively modulate the response of the T cell ([36]). This function is believed to be of particular importance with respect to cancer because it makes it possible to define a threshold value for presentations of an antigen. Absent the inhibitory receptors, T cells which can attack cancerous cells expressing an abnormal amount of a normal antigen will also attack non-cancerous cells presenting normal amounts of the same antigen, although weakly. With the inhibitory receptor, T cells can compare the expression of the antigen to the inhibitory receptor signal and react only if the antigen expression passes a threshold, thus avoiding the attack on non-cancerous cells which are below threshold. The TCR of these T cells having inhibitory receptors is affected by electromagnetic waves like all TCRs, but there is no clear indication that the inhibitory receptors may be affected. Assuming that in most cases inhibitory receptors are un-affected, T cells having inhibitory receptors react to an artificial wave causing an inhibitory effect (INH) by a diminished binding capability, like "simple" T cells, and their selection by the thymus in the presence of artificial electromagnetic waves yields abnormally aggressive T cells, as is the case with "normal" T cells. However, if any inhibitory receptor is inhibited by electromagnetic waves in a manner comparable to a TCR, this inhibition will result in an anti-cancer effect after a low to high transition instead of the pro-cancer effect predicted by Table "INH+ENS" of Figure 8.

2.6.3 Intermediate mechanisms modulating the decision-making capabilities of a TCR

As discussed in section 2.6.2, in T cells which have inhibitory receptors, such receptors may collaborate with TCRs in defining a threshold in the number of presentations of a self antigen which are considered as abnormal, so as to trigger an immune response based not only on the nature (self or non-self) of an antigen, but also on the number of presentations of this antigen. The mechanism for such collaboration must be at the level of the cell rather than of an individual TCR. For example, the isolated recognition of an antigen by a TCR, rather than directly triggering the attack of the T cell on the APC, may rather trigger a signalling event, with another internal cellular mechanism being able to essentially substract a weighted number of inhibitory receptor signalling events from a weighted number of TCR signalling events to reach a decision threshold. At least in this case, there are therefore intermediate mechanisms modulating the decision-making capabilities of a single TCR. Also, whilst it has been generally assumed herein that the recognition takes place in each TCR-pMHC system, this assumption may be a simplification of reality and other cell components may be implied and may need be included in the system to properly define the quantum wells.

2.6.4 Effects on B cells

B cells start antibody production when they detect a corresponding antigen and receive a "confirmation" signal which may come from a T cell. Thus B cells are at least affected via the T cells. It is unclear at this stage whether or not the direct recognition of the antigen by the B cell is based on the same mechanism as the recognition by the T cell and whether or not it can be inhibited by an electromagnetic wave in the same frequency range which affects the T cells.

2.6.5 Influence of pre-existing artificial electromagnetic waves

The effects of a change in the electromagnetic environment depends not only on the added electromagnetic wave, but also on the pre-existing electromagnetic waves. For example, a pro-cancer effect is expected to be lower if the power density of an existing artificial wave is increased than if a new artificial wave is introduced on a thermal background. Generally, the effects of any specific artificial electromagnetic wave occupying a defined part of the frequency spectrum cannot be considered separately

from the effects of other electromagnetic waves occupying other parts of the frequency spectrum, because they may all contribute to transitions in the same TCR-pMHC systems. Therefore, the exact prediction of the effects of an added electromagnetic wave goes beyond the sole principles of Table "INH+ENS" of Figure 8. Table "INH+ENS" is expected to apply when the "low exposure" condition is the thermal background, but the situation becomes more complex when various electromagnetic waves of different frequencies and bandwidths interact with each other. In such complex situations, Table "INH+ENS" is expected to apply in many cases, but not all cases.

2.6.6 Interaction of the immune system with developmental timing

A factual finding in section 3.1.4 is that a lack of immunity results in a disturbance of developmental timing. A possible explanation is that the lack of immunity results in survival of "abnormal" cells and thus a disturbance of developmental timing. However, the interaction of the immune system with developmental timing may go further than that. I propose that during early phases of postnatal development, antigens are progressively suppressed from the negative selection section of the thymus. Suppressing an antigen from the negative selection section of the thymus implies that T cells targeted to this antigen are allowed to survive negative selection and therefore outside the thymus cells bearing this antigen start to be eliminated by the immune system. If cells (say, cells "C") bearing this antigen ("developmental antigen") are involved in a phase of the development but not in the next phase, elimination of the antigen from the pool of antigens presented in the thymus results in eliminating these cells "C" and thus triggers the "next phase" of development.

In [3] exposure to the immuno-suppressant cyclosporin delayed developmental timing endpoints and increased their standard deviation. In [7] permanent exposure to strong electromagnetic waves increased the standard deviation of developmental timing endpoints but did not delay them. This difference can be understood by assuming that :

(i) developmental antigens behave as "near-self" after their suppression from the pool of antigens implied in thymus selection, so that T cells recognizing them react essentially like T cells implied in cancer or auto-immune diseases.

(ii) cyclosporin does not affect thymus selection (but exposure to electromagnetic waves does).

In the case of cyclosporin, the average affinity of T cells for the developmental antigens is reduced, so any T cell line capable of recognizing these antigens will be slower in eliminating the "C" cell lines bearing developmental antigens. This causes a delay in the corresponding developmental timing endpoints. In the case of exposure to electromagnetic waves, negative thymus selection in the exposed situation allows more T cells to survive and globally equilibrates the affinity of T cells for developmental antigens. Therefore the time needed for a T cell line to eliminate a "C" cell line is un-modified, and the developmental timing endpoint is not delayed.

In the case of cyclosporin, the number of naive T cells capable of recognizing a "C" cell line is reduced because cyclosporin causes many T cells to become unable to recognize the developmental antigen. In the case of exposure to (relatively strong) electromagnetic waves, the number of naive T cells able to recognize developmental antigens is reduced because positive selection eliminates many T cells and in the power range implied results in a net reduction of the number of surviving T cells. In either case, the reduction in the number of naive T cells capable of recognizing the "C" cell line bearing the developmental antigen results in the chance factor playing more heavily in determining the efficiency of the specific T cell line which will be cloned to eliminate a "C" cell line, and therefore in an increase of the variance of the developmental timing endpoints.

If the above reasoning is correct, it should also apply to variations of auto-immunity which occur due to low-power, large-bandwidth electromagnetic waves, corresponding to Table "INH+ENS" of figure 8.. In the case of column C of Table "INH+ENS", there is lack of immunity caused by a decrease of the aggressiveness of T cells which during the transition period is not compensated by the thymus. This is expected to result in less efficiency of any cloned T cell line eliminating a "C" cell line, and thus cause a delaying in any affected developmental timing endpoints. Similarly, in the cases of column "D" or "E" an acceleration of developmental timing is expected. The acceleration of developmental timing may be limited because a developmental timing endpoint cannot occur earlier than the elimination of the corresponding developmental antigen from the pool of antigens presented during negative thymus selection.

2.7 Discussion of the restriction $\Omega_b >> \Omega_c$ in the Recognition Mechanism

This restriction of the recognition model (RE) implies that (at least in the absence of artificial electromagnetic waves) the TCR binds best to the pMHC when Ω_b is lowest, i.e. when it has the lesser tendency to move from quantum well (a) to quantum well (b). This is somewhat counter-intuitive as one would expect TCRs which go faster into quantum well (b) to also go faster into quantum well (c) and thus to best bind the pMHC, as would actually be the case with $\Omega_b < \Omega_c$.

This can be best understood using a 3D picture as shown on figure 9. Quantum wells (a) and (b) are limited inter alia by a strong energy barrier and separated from each other by a weaker energy barrier ("passage"). The minimum energy path passes through the weaker energy barrier. In order to efficiently block passage between the two quantum wells, the peptide must have exactly the shape of the passage left by the stronger energy barriers, otherwise if the peptide "is too small" an alternate minimum energy path can bypass it without crossing the strong energy barrier or if the peptide "is too large" it cannot fit in the passage so that there is also a minimum energy path through the passage which does not cross the strong energy barrier. When the peptide blocks the passage efficiently the barrier between quantum wells (a) and (b) becomes stronger and the Ω_b is significantly reduced

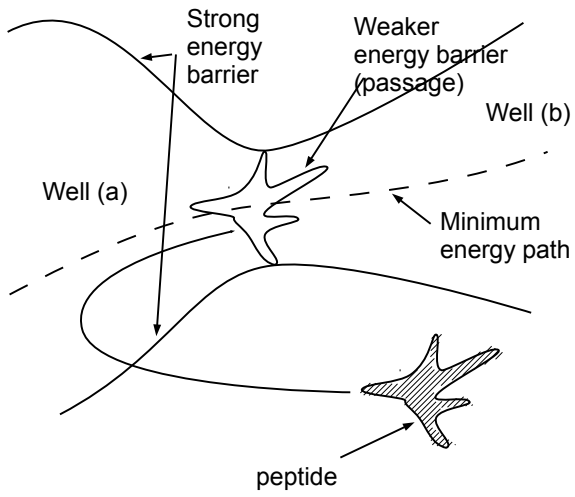

Figure 9: a 3D picture of a mechanism of peptide recognition.

so the peptide is "recognized" and the system goes into non-represented well (c). So the mechanism makes it possible to differentiate even between similar peptides based on their capacity to block the passage between the quantum wells, which is determined by steric effects.

The reality is in many dimensions and is a lot more complex than that, but this simple picture helps in understanding that a mechanism based on blocking a minimum energy path (as is the case when $\Omega_b > \Omega_c$) may be a lot more specific than a mechanism based on accelerating transitions between two quantum wells (as would be the case with $\Omega_b < \Omega_c$). The capacity to accelerate a transfer from well (a) to well (b) relies essentially on electrostatic attraction, whilst the capacity to block an existing path relies essentially on steric effects. The capacity to block a path (under the hypothesis $\Omega_b > \Omega_c$) is like the capacity of a mechanical piece to block a flow of water in a conduit: the mechanical piece must have exactly the right shape. The capacity to accelerate a path (under the hypothesis $\Omega_b < \Omega_c$)is like the capacity of two magnets to attract each other. The blocking test is much more specific.

This simplistic argumentation is not a full justification but it helps in understanding why this specific binding principle, including the restriction $\Omega_b > \Omega_c$, is probably advantageous for living organisms (because it is more specific) and has been selected through evolution.

Whilst recognition of a threat pursuant to the recognition mechanism (RE) needs to be highly specific because otherwise the immune system could attack the self unnecessarily, causing auto-immune problems, the non-recognition mechanism (NRE) which triggers temporary inactivation (TI) does not potentially result in direct damages to normal cells and therefore needs not be as specific, so that the opposite condition $\Omega_{b'} > \Omega_{c'}$ is acceptable for the non-recognition mechanism (NRE).

3 Discussion of experimental results

3.1 Effects of electromagnetic waves below 3 GHz

3.1.1 Cancer-promoting effect of high-power temporary exposures

In [78] exposure to a 2450 MHz cw wave at 50, 100 or 150 W/m2 2h daily 6 days/week for 1 to 6 months, prior to (100 W/m2) or during (50 or 150 W/m2) cancer development, accelerated the development of benzopyrene-induced skin cancer in mice.

The results in [78] can be interpreted as follows:

- as discussed in section 2.4.3 a cw artificial wave can temporarily inactivate T cells (INA). This mechanism is favoured as compared to the inhibition (INH) of section 2.2.2 by the fact that the wave is cw rather than large-bandwidth.

-Outside the thymus, the inactivation of T cells directly creates a short-term pro-cancer effect. Further, repeated inactivations of the same T-cells may result in apoptosis of these T cells yielding a long-term pro-cancer effect.

-In the thymus, the same process yields elimination of T cells as described in section 2.4.2. If the inhibition is strong enough, T cells which would otherwise be efficient against cancer can be eliminated as discussed in section 2.4.4. This yields a delayed, longer term pro-cancer effect which explains the pro-cancer effect observed on mice exposed to microwaves prior to being exposed to cancer-promoting chemicals.

Thus, the pro-cancer effect observed can be explained on the basis of the temporary inactivation effect (INA) pursuant to the non-recognition mechanism (NRE). Experimental results in this specific case show the pro-cancer effect increasing very significantly between 50 W/m2 and 150 W/m2 with a threshold for this effect which is probably little less than 50 W/m2. The fact that the effect is increasing between 50 W/m2 and 150 W/m2 is also confirmation that the value of $\Omega_{b'}$ under exposed conditions remained lower than $\Omega_{c'}$, since otherwise the effect would have decreased with increasing power density.

Essentially the same results as in [78] were also obtained in [66] with a pulsed 900 MHz field with instantaneous power density between 20 and 100 W/m2. Importantly, in [78] and [66] the exposed group was compared with a sham-exposed group, and the exposed and sham-exposed group staid for the same durations in anechoic chambers.

3.1.2 In vitro temporary inactivation of T cells

In [52] the inhibition of the recognition of a target cell by a T cell line was directly observed in a cytotoxicity assay. The artificial electromagnetic wave was a 15 W/m2, 450 MHz field sinusoidally amplitude modulated at 60 Hz. Effects at lower modulation frequency diminished progressively and no effect was observed on the un-modulated carrier. Effects at 80 or 100 Hz were also smaller than at 60 Hz. No effect was found for the unmodulated carrier. The inhibitory effect was observable when the cytotoxicity effect was simultaneous with the exposure, but it was also

observable when exposure happened prior to the cytotoxicity assay.

If the sole observed effect had been due to the "recognition" mechanism (RE) of section 2.2, it should not have been observable when exposure happened prior to the cytotoxicity assay. Thus the observed effect was probably due mainly to the "non-recognition" (NRE) mechanism of section 2.4, applied to the recognition of self antigens by the effector T cells. This is also consistent with the fact that an essentially cw wave was used, which as discussed in section 2.4 may have a stronger effect on the non-recognition mechanism (NRE) than on the recognition mechanism (RE).

However the 450 MHz un-modulated wave did not yield a detectable inhibition, whilst the modulated wave did. A proposed explanation for this is as follows:

The efficiency of the temporary inactivation (INA) caused by a cw wave is dependent on the existence of sufficient thermal relaxation within well (a). In the present case - corresponding to the specific T cell line being studied - thermal relaxation mechanisms may have been insufficient when the sole 450 MHz carrier was present, preventing significant temporary inactivations to occur.

Quantum well (a) may be weakly interacting with a further quantum well (d) having a near-continuum of quantum states. If the frequency step between quantum states in well (a) is 120 Hz, the 60 Hz modulated carrier can cause a quantum state in (a) to interact with its neighbouring quantum state in well (a) via a quantum state of intermediate frequency (i.e.energy) in well(d). It can thus cause accelerated transitions between quantum states in well (a), which is a substitute for strictly thermal relaxation.

Assuming that the temporary inactivation effect (INA) was limited in the case of the sole 450 MHz carrier by the insufficient thermal relaxation, the 60 Hz modulation which accelerates transitions between quantum states of well (a) removes this limitation and allows transfers between wells (a) and (b) to proceed, yielding a significant temporary inactivation effect (INA).

This effect of the 60 Hz modulation could be observed because the frequency generator had a good frequency stability. If a generator with a lesser frequency stability is used, the stimulated transitions via well (d) may take place without any on-purpose modulation, because the generator's frequency changes over time. It is thus somewhat unclear whether the same sort of stimulated transitions via well (d) also played a role in the "in vivo" experiment in [78] or whether thermal relaxation was sufficient as of itself.

3.1.3 Auto-immunity: confirmation studies of Russian and Ukrainian data

Two essentially identical experiments were carried out, respectively in Russia [29] and in France [16]. Rats were exposed 7 hours daily 5 days/week during a 30 days period, to 2450 MHz cw at 5 W/m2. The sham and RF-exposure groups were both installed in shielded anechoic chambers, i.e. Faraday cages. The cage controls were not. The results of the two experiences were different. To understand these experiments and the discrepancies between results I will consider the following extreme cases:

(A) The environmental exposure is null (corresponding to Table "INH+ENS" column A on Figure 8).

(B) The environmental exposure is a large-bandwidth, low power density permanent wave (corresponding to Table "INH+ENS" column B).

Generally, the environmental exposure is considered as having direct inhibitory effects (INH , ruled by Table "INH+ENS") because of its large bandwidth and low power density. The 2450 MHz exposure is a cw exposure more likely to cause temporary inactivations (INA) by the non-recognition mechanism (NRE) than to cause the inhibitory effect (INH) by the recognition mechanism (RE). It is therefore likely that its dominant effect is an effect of temporary inactivation (INA). This is also confirmed by the fact that the effect in a similar experience (although at 0.5 W/m2) in [20] (reported in [65] and [27]) did find a decrease in antibody response for rabbits exposed during or before sensitization. If the effect had been based on the inhibitory effect (INH) which is assumed to be instantaneous, a 4 hours/day exposure would have caused a pro-auto-immune effect as per Table "INH+ENS" column E but would not have caused a significantly diminished antibody response to non-self, because there were 20 hours/day of normal response to non-self.

In case (A) the entry into the Faraday cages has no effect. The exposure to the 2450 MHz wave inactivates a number of T cells. Typically inactivation lasts for 12 hours as discussed in section 3.1.2 , which is of the same order of the time period separating successive 7-hour exposures in [29] [16]. Therefore a number of T cells are permanently inactivated during the 30 days period (except possibly during the 2 days/week of non-exposure).

The effect of temporary inactivations (INA) on thymus selection yields after the end of the 30-day period to a pro-auto-immune effect essentially as described in section 2.4.4. A T cell precursor which undergoes positive selection during a non-exposure period (i.e. 17 hours/day) may become temporarily inactivated (INA) during its transit through the positive selection part of the thymus, thereby escaping negative selection. T cells which escaped negative selection in this manner are expected to remain inactivated essentially for the full 30 days of exposure. However, when exposure ceases, these T cells are activated again and since they have escaped negative selection, they cause a pro-auto-immune effect, lasting until they become eliminated by extra-thymic regulation mechanisms. The non-exposure 2 days per week during the 30-day period somewhat mitigates this and causes a limited auto-immune effect even before the end of the 30-day period. So there is a very limited auto-immune effect during the 2 day/week non-exposures, but the bulk of the pro-auto-immune effect is delayed until the end of the 30-day period.

In case (B), the entry into the Faraday cages results in a pro-auto-immune effect as per Table "INH+ENS" column D and in a reduction of the number of T cells which are inactivated by the temporary inactivation effect (INA) which is expected to take place both for cw or wideband exposure. The exposure to the 2450 MHz cw wave results in an increase in the number of T cells which are temporarily inactivated. However this increase may es-

sentially mitigate the decrease due to entry into the Faraday cage. After the end of the 30-day period, the T cells which were inactivated during their transit through the positive selection part of the thymus due to the 2450 MHz exposure remain inactivated due to the environmental exposure (and ultimately may undergo apoptosis), so that they do not cause any increase of auto-immunity. The T-cells which did undergo some positive selection steps during the non-exposed periods (17h/day) within the 30-day period undergo an anti-auto-immune transition as per Table "INH+ENS" column D.

Important differences between cases (A) or (B) are as follows:

In case (A) there is a pro-auto-immune period after termination of the 30-day period, for the exposed group relative to both the sham-exposed group and the control group. In case (B) there is an anti-auto-immune period after termination of the 30-day period, for both the sham-exposed and the exposed group.

Real situations may tend towards case (A) or case (B) and may be further complicated by the presence of time-varying waves.

In [29] at day 7, the ELISA test based on blood serum yielded a significant increase of the amount of 5 groups of antibodies in the exposed group relative to the sham group [28]. The fact that the exposed group had more antibodies than the sham group is characteristic of case (A) and attributable to the pro-auto-immune period taking place after the end of the 30-day period. At day 14 the differences in antibody amount between the exposed and sham-exposed group were not significant except for one group of antibodies, for which it was not significant at day 7. This may reflect the temporary nature of the pro-auto-immune period taking place after the 30-day period in case (A). The antibody amount in the sham group was generally higher than in the control group and this may be due to the fact that the case is intermediate between (A) and (B), with the higher antibody amount in the sham group reflecting the pro-auto-immune conditions during the 30-day period, taking into account the fact that antibodies have a certain lifetime in blood (estimated to 20 days in [6]). In the brain, antibody contents is expected to reflect changes in blood antibody contents with a delay due to buffering and to the blood-brain barrier. Complement Fixation Test (CFT) analysis of brain tissues determined that in the brain the increase of antibody contents was equal (although not significant) for the sham and exposed group at day 7, possibly reflecting the (earlier and characteristic of case B) pro-auto-immune effect of entering the Faraday cage, and was significantly higher in the exposed group than in the sham-exposed group at day 14, possibly reflecting the (later and characteristic of case A) pro-auto-immune effect due to end of the 30-day period.

In [16] the complete results of an ELISA test implying 48 antibodies were published as supplementary material. I re-interpreted these results as shown in Table 1.

These re-interpreted results show that at day 14 the antibody contents was higher in the control group relative to the two other groups, probably reflecting the anti-auto-immune period occurring in case (B) after the end of the 30-day period. They also show that:

(a) the variance of the antibody contents was higher in the sham group than in the control group at day 7. This is most likely attributable to the following facts: the auto-immune effect of entering a Faraday cage generally affects only certain T cells, i.e. those which were previously affected by the environmental background of artificial electromagnetic waves, for example due to an appropriate bandwidth condition. Thus, within the T cells which can trigger production of a specific antibody, some (in some animals) may react to an auto-immune effect yielding abnormally high optical densities, and others not (inter alia, in other animals). Therefore, the auto-immune effect of entering the Faraday cage first causes a spread of the antibody response, i.e. an increase of variance. The averages may also react, but less significantly. This spread is higher at day 7 when antibodies produced during the 30-day period are still dominating, than at day 14 when antibodies produced during the 30-day period are in lesser amounts.

(b) the variance of the antibody contents was lower in the sham group than in the control group at day 14. This is most likely attributable to the following facts: after leaving the Faraday cage, the T cells of the sham group which had become abnormally aggressive at entering the Faraday cage behave normally again, suppressing the spread of the antibody response which was initially due to entering the Faraday cage. The T cells thymus-selected during the 30-day period become less aggressive, so that their contribution to immunity is low. Recent thymus emigrants generally provide the most aggressive T cells before their elimination by the regulatory mechanisms discussed in section 2.6.1, and in this case the recent thymus emigrants have abnormally low aggressiveness. Thus the number of highly aggressive T cells is abnormally low, which determines both a decrease in antibody contents and a decrease in variance of the antibody contents. Since this effect is triggered by leaving the Faraday cage, it dominates over the effect described in (a) at day 14 when antibodies produced after leaving the Faraday cage dominate over antibodies produced whilst being in the Faraday cage.

(c) the variance was lower in the exposed group than in the sham group. A proposed explanation for this is as follows: The pro- autoimmune [resp. anti-auto-immune] effects of entering [resp. leaving] the Faraday cage is due to the inhibition effect (INH). It affects only T cells with certain Δ_b values determined by the bandwidth condition of equation 6. These effects are accompanied by increases in variance due to the difference between affected and non-affected T cells. The effects whether pro or anti-auto-immune of temporary inhibition (INA) affect a wider range of T cells because they are not limited by a bandwidth condition. Thus the effects of temporary inactivation (INA) do not necessarily cause an increase of variance, and may even reduce the variance when they mitigate some effects of temporary inhibition (INH). Where the effects of (INA) and of (INH) are mixed as is the case in the exposed group, the variance is thus expected to be lower than when the sole effects of (INH) exist.

The discrepancies between the results of [29] and [16] would thus be due to the fact that in [29] the situation

		7 days			14 days		
		>0	<0	(>0)-(<0)	>0	<0	(>0)-(<0)
Optical Densities	Control – Exposed	6**(a)	3 (b)	3 (c)	7**	2	5*
	Exposed - Sham	4	1	3	4	3	1
	Control - Sham	0	3	-3	8***	1	7**
	order	Exposed<Control			Sham=Exposed<Control		
		>1	<1	(>1)-(<1)	>1	<1	(>1)-(<1)
Variances of OD	Control / Exposed	11***(d)	6**(e)	5*(f)	21***	3	18***
	Exposed / Sham	2	12***	-10***	4	8***	-4*
	Control /Sham	3	8***	-5*	13***	5*	8***
	order	Exposed<Control<Sham (g)			Exposed<Sham<Control		

Table 1: ELISA test results in [16]. (a): number of ELISA test results in which the optical density for the control group is significantly ($p < 0.05$) higher than the optical density for the exposed group, tests made at 7th day of life. (b): number of ELISA test results in which the optical density for the control group is significantly ($p < 0.05$) lower than the optical density for the exposed group, tests made at 7th day of life. (c): difference (a) -(b). (d): number of ELISA test results in which the variance of the optical density for the control group is significantly ($p < 0.05$) higher than the optical density for the exposed group, tests made at 7th day of life. (e): number of ELISA test results in which the variance of the optical density for the control group is significantly ($p < 0.05$) lower than the optical density for the exposed group, tests made at 7th day of life. (f): difference (d) -(e). (g): groups ranked from smallest to highest variance. Other items have similar definitions in accordance with line and column titles. *: number is significant to $p < 0.05$. **:number is significant to $p < 0.01$. ***:number is significant to $p < 0.001$. Significance of the differences between groups in each ELISA test results was assessed based on a z-test (for average optical densities) and based on an f-test of equality of variances (for variances). Significance of the numbers shown for example in (a) and (b) is assessed using a cumulative binomial law. Significance of the differences shown for example in (c) is appropriately derived from a binomial law. Total number of ELISA tests per group is 48.

was intermediate between cases (A) and (B) (i.e. there was a relatively low artificial environmental background) whilst in [16] the situation was typical of case (B) (i.e. the experimental results were dominated by the effects of a strong environmental background).

The experience [29] also comprised a teratological test. In this teratological test serum from rats of the sham [resp. exposed] group was injected to pregnant females (hereafter the "sham" [resp. exposed] group of pregnant females. A control group of females was not injected with serum. A strong effect on intra-uterine death was found for the exposed group relative to the sham and control groups. This effect was not reproduced in [16] and this is likely attributable to the fact that in [16] the exposure group had a lower antibody contents than the other groups, rather than higher in [29].

Thus the results in [16] after re-interpretation are highly significant and the difference between [16] and [29] is probably due to the presence of more environmental electromagnetic background in [16] than in [29].

3.1.4 Auto-immunity: Multi-generation studies

In [9] [10] [79] [7] various developmental timing endpoints were investigated in multi-generational studies in rats. To assess whether reported variations in the standard deviation of these parameters were significant, i made an f-test of equality of variances. I calculated f-numbers (variance in the exposed group divided by variance in the sham group) and determined a level of significance based on the number of litters (applying the one-sided F distribution test with the number of litters as degrees of freedom). The results are presented in Table 2.

The cases of [79] (TAK) is clear-cut. A significant increase of the variance of the vaginal opening day ($p < 0.1$) and of the variance of the balanopreputial cleavage day ($p < 0.025$) were obtained in the highest exposure group. A non-significant increase of the variance of the vaginal opening day and a significant variance of the balanopreputial cleavage day ($p < 0.025$) were obtained in the lowest exposure group.

The results of [7] (MUN) are also clear-cut, with much stronger f-values.

In order to further assess the significance of the results in [7] and [79] i conducted an examination of randomly chosen multi-generational studies relating to exposure to chemicals, on the same basis. The F-numbers obtained for balanopreputial cleavage in [79] and for eyes opening in [7] are unequaled in any of the randomly chosen examples of Tables 3 and 4 . The same can essentially be said of all significant f-numbers concerning developmental timing endpoints investigated in [7]. For completeness, Table 5 shows the original standard deviation data for the "eyes opening" parameter. The results in [7] and [79], in addition to being mathematically significant, are thus clearly not within the normal range for this sort of multi-generational studies.

The wave used in [7] for UMTS was a time-variable realistic simulation with a bandwidth of about 5 MHz [61]. The wave used in [7] for GSM was a single GSM frequency with all time slots filled with random data and was thus

				standard deviation (power density W/m2 ; SAR W/kg)				f-number [p-value]	
Endpoint	exposure of parental generation	Exp. type	Pub. Ref.	shelf	sham	low exposure	high exposure	low exposure	high exposure
vaginal opening	part of life 20h/day	UMTS	[9]	1.93	1.73	2.21 (3.2;0.16)	1.44 (32;1.6)	1.63	0.69
			[10]	2.63	1.83	2.62 (3.2;0.16)	1.68 (32;1.6)	2.05[0.05]	0.84
	Lifelong	CDMA	[79]		1.9	2.3 (1.6?;0.04)	2.9 (3.5?;0.08)	1.47	2.33[0.1]
balano - preputial cleavage	part of life 20h/day	UMTS	[9]	2.30	2.23	1.73 (3.2;0.16)	1.35 (32;1.6)	0.6	0.37[0.01]
			[10]	1.18	1.1	1.18 (3.2;0.16)	1.37 (32;1.6)	1.15	1.55
	Lifelong	CDMA	[79]		1.8	3.4 (1.6?;0.04)	3.5 (3.5?;0.08)	3.57[0.025]	3.78[0.025]
eye opening	Lifelong	UMTS	[7]		0.29	1.03 (29;0.4)		12 [0.01]	
	22h/day	GSM	[7]		0.29	5.1 (28;0.4)		309 [0.01]	
ear opening	Lifelong	UMTS	[7]		0.4	2.21 (29;0.4)		30 [0.01]	
	22h/day	GSM	[7]		0.4	3.92 (28;0.4)		96 [0.01]	
incisor eruption	Lifelong	UMTS	[7]		0.77	0.75 (29;0.4)		0.95	
	22h/day	GSM	[7]		0.77	2.82 (28;0.4)		13 [0.01]	

Table 2: Developmental timing endpoints in multi-generational studies. power density for [79] is evaluated from exposure data in W/kg based on average proportions of [9] and [7]. In [9] exposure started 10 weeks before mating, in [10] it started after successful mating. N=12 in [7] and [79], N=24 in [9], N=23 to 25 in [10]
.

reference/product/other	exp 1	exp 2	exp 3	exp 4	exp 5
[22] DBCS rubber accelerator- F1 males	0.69	0.69	0.69		
[22] DBCS- F1 females	1.36	0.44	0.69		
[22] DBCS- F2 males	1.31	1	0.73		
[22] DBCS- F2 females	1.78	0.69	1.36		
[21] A -F1 males	1.96	1.96	2.56	1.44	
[21] bisphenol A F1 females	1.36	1.36	1.78	1	
[21] bisphenol A F2 males	1.31	1	1	0.73	
[21] bisphenol A F2 females	1.31	1	0.73	0.51	
[81] toluene	0.85	1.47	0.88	1.17	
[41] zinc male	1	1	1.82		
[41] zinc female	1	1	1.44		
[33] MDMA	1				
[51] dibutyl phthalate	1.18	2.25	2.52	1.12	
[62] levetiracetam	1.78	1	3.36	0	
[15] pesticides	1.35	1.71	1.4	2.35	1.44
[70] - cadmium	6.89				
[43] styrene	0.86	1.15			
[13] trichloroethane	1				

Table 3: F-numbers for exposure to chemicals for endpoint "eye opening day" in rats.

reference/product/other	exp 1	exp 2	exp 3	exp 4
[59] phthalate	1	1	2.35	0
[35] isodecyl phthalate F1	0.55	0.76	0.55	0.91
[35] isodecyl phthalate F2	0.33	0.46	0.51	0.86
[25] ethyl butyl	0.42	0.78	0.89	
[60] nonylphenol	0.82	0.82	1.1	
[74] D5 vapor-F1	2.75	1.8	1.4	
[74] D5 vapor-F2	1.06	0.57	0.55	
[73] D4 vapor F1	1.04	0.55	0.65	1
[73] D4 vapor F2a	1.5	1.35	1.84	2.01
[30] styrene	1.47	1	1.31	
[86] alkyl phthalate- D79P	1	1.73	1.87	
[86] alkyl phthalate- D911P	1.18	1.38	1.48	

Table 4: F-numbers for exposure to chemicals for endpoint "balanopreputial cleavage day" in rats.

very similar to a permanent random noise of 200 kHz bandwidth. Since the latter yielded a stronger effect on developmental timing endpoints, the following discussion will be based on it. Due to the 200 kHz bandwidth and gaussian-noise-like characteristics of the signal, the signal could potentially trigger an inhibitory effect (INH) as discussed in section 2.2.2. Since the power density is in the range of power densities which in [78] caused a significant pro-cancer effect based on an inactivatory effect (INA), the signal could also trigger a significant inactivatory effect (INA). However, the effect was stronger for GSM, which had a lower bandwidth and a less time-varying signal, than for UMTS which had a larger bandwidth and more time variations. Since the inhibitory effect (INH) is expected to be stronger for the larger bandwidth of UMTS and to cause more pro-auto-immune effects due to the stronger time variations of UMTS, the fact that the effect was actually stronger for GSM than for UMTS is a strong in-

reference	sham	exp 1	exp 2	exp 3	exp 4	exp 5
[22] DBCS rubber accelerator- F1 males	0.6	0.5	0.5	0.5		
[22] DBCS- F1 females	0.6	0.7	0.4	0.5		
[22] DBCS- F2 males	0.7	0.8	0.7	0.6		
[22] DBCS- F2 females	0.6	0.8	0.5	0.7		
[21] bisphenol A -F1 males	0.5	0.7	0.7	0.8	0.6	
[21] bisphenol A F1 females	0.6	0.7	0.7	0.8	0.6	
[21] - bisphenol A F2 males	0.7	0.8	0.7	0.7	0.6	
[21] - bisphenol A F2 females	0.7	0.8	0.7	0.6	0.5	
[81] toluene	0.83	0.77	1.01	0.78	0.9	
[41] zinc male	0.2	0.2	0.2	0.27		
[41] zinc female	0.2	0.2	0.2	0.24		
[33] MDMA	0.2	0.2				
[51] dibutyl phthalate	0.34	0.37	0.51	0.54	0.36	
[62] levetiracetam	0.6	0.8	0.6	1.1		
[15] pesticides	0.84	0.98	1.1	0.99	1.29	1.01
[70] - cadmium	0.16	0.42				
[43] styrene	1.4	1.3	1.5			
[13] trichloroethane	0.3	0.3				

Table 5: Standard deviations for exposure to chemicals for endpoint "eye opening day" in rats .

reference/product/other	exp 1	exp 2	exp 3	exp 4
[59] phthalate	3.19	2.04	2.25	
[83] estradiol	0.64	0.49	0.22	
[35] isodecyl phthalate F1-A	2.25	4	2.69	
[35] isodecyl phthalate F1-B	2.64	2.25	4	2.25
[35] isodecyl phthalate F2-B	1	0.66	1.19	1.61
[25] ethyl butyl	1.47	2.46	2.25	
[60] nonylphenol	0.64	1.25	0.52	
[34] aluminium sulfate	0.65			
[74] D5 vapor-F1	2.04	1.234	1.28	
[74] D5 vapor-F2	0.70	0.56	1.35	
[73] D4 vapor F1	1	0.65	0.88	0.84
[73] D4 vapor F2a	0.62	2.04	1	1.65
[30] styrene	0.85	0.70	0.85	
[86] alkyl phthalate-D79P	1.67	1.99	1.25	
[86] alkyl phthalate-D911P	1.32	2.72	1.21	

Table 6: F-numbers for exposure to chemicals for endpoint "vaginal opening day" in rats.

dication that it was not based on a pro-auto-immune or inhibitory effect (INH) but rather on an inactivatory effect (INA). This raises the question of whether this inactivatory effect may have caused the observed disturbance of developmental timing endpoints.

It is at least conceivable that auto-immunity of the pups partly regulates developmental timing endpoints by deciding which cells are or are not eliminated by the immune system. This issue is discussed in more detail in section 2.6.6. It is similarly conceivable that lack of immunity in the mothers resulted in less resorptions and therefore more surviving foetuses which would otherwise have been eliminated due to slight deviations from normality.

In [9] and [10] , unlike [7] and [79], the parental generation was not exposed lifelong and there is no assessment of environmental exposure prior to start of the experience. Therefore, auto-immune effects on the parental generation at entering the Faraday cage must be taken into account. This auto-immune effect had the opposite result as compared to the lack of immunity in [7] [79] resulting in a lower standard variation of developmental timing endpoints in the sham group than in the control group. This fact also indirectly confirms the link between lack of immunity of the mothers and disturbances of developmental timing of the offspring.

This link is also confirmed in [50] which is a multigenerational study on 4 generations, in which the first generation showed abnormal, power density-dependent variations of the number of malformed fetuses (a parameter expected to be related to the developmental timing endpoints in [7]). More specifically, the number of malformed fetuses showed a minimum for the sham group, followed by a maximum for the lowest exposure group, then a further minimum for the intermediate exposure group and a further maximum for the highest exposure group. These maximums and minimums were significant, and were not reproduced in the next generations. The minimum number of malformed foetuses in the sham group was also accompanied by a maximum number of resorptions in this sham group. These facts confirm the higher number of resorptions and lower number of malformed foetuses corresponding to the stronger immunity in the first parental generation due to entering the Faraday cage. Thus they also indirectly confirm the opposite effect of a higher number of abnormalities in foetuses in case of a lack of immunity.

The link between lack of immunity and disturbance of developmental timing is further confirmed by the fact that exposure to the immuno-suppressor cyclosporin also yields abnormal f-numbers in [3] as shown in Table 7. The f-number for vaginal opening is higher than any of the randomly chosen f-numbers in Table 6 for vaginal opening. The f-number for incisor eruption is also abnormally high. Further, in [3] the cyclosporin was not given to the mothers but only to the pups, so that this experimental result specifically confirms the link between lack of autoimmunity of the pups (as opposed to the mothers) and the disturbance of developmental timing endpoints.

So altogether, the reactions of the first generation of offspring in the sham groups after entry in the Faraday cage of the parental generation in [50] [9] [10] and the reaction to the immuno-suppressor cyclosporin [3] largely confirm the link between lack of immunity and disturbance of developmental timing endpoints observable in [79] [7].

Therefore the preferred hypothesis for explaining the observed disturbance of developmental timing endpoints in [79] [7] is thus that it caused an insufficient autoimmunity to arise due to the inactivatory effect (INA).

In [10] low exposure resulted in an increase of the standard deviation relative to sham, essentially cancelling the

endpoint	f	N(min)	p<
Incisor eruption	3.33 (a)	58	0.01
Eye opening	2.15 (a)	57	0.01
Vaginal opening	9.43 (b)	14	0.01
Balano-preputial cleavage	0.28 (b)	13	0.025

Table 7: F-numbers for exposure of newborn rats from day 4 to day 28 to 10 mg/kg cyclosporin [3] and one-sided p-values. (a) f-number based on standard deviation of the normal distribution which best fits the published percentages of pups positive on two given days. (b) f-number based on published standard deviations.

diminished standard variation of developmental timing endpoints due to entering the Faraday cage. But in [9] for balanopreputial cleavage day, high exposure resulted in a significant decrease of the standard deviation which at first sight is difficult to explain; but the fact that this sort of behaviour is specific to the first generation is confirmed by comparison with [50] in which the intermediate exposure group had a lower number of malformed foetuses than the lowest exposure group, which in [9] [10] would correspond to a standard deviation of developmental timing endpoints, as observed.

The abnormal decrease of the variance for high exposure in [9] and is thus known to be due to the effect on the parental animals of entering the Faraday cage, combined with the effect of exposure, and not to exposure alone. It is probably due to a specific interaction between mechanisms (INA) triggered by exposure, (INH) triggered by entering the Faraday cage, and positive (EPS) and negative (ENS) thymus selection.

In short, multi-generational studies in which the parental generation was exposed for its entire lifetime consistently showed increases of the standard deviation of the dates of various developmental steps of the rats, most likely attributable to a temporary inactivation (INA) of T cells in the progeny and/or the parental generation. Where the parental generation was only exposed from mating, the combination of pro-auto-immune effects of entering the Faraday cage and of the inactivatory effect (INA) produced a power density-dependent behaviour of increase or decrease of standard deviation with respect to power density.

3.1.5 Decreased incidence of brain cancer in moderate cellular phone users

In the United states before 1998 the cell phone market was dominated by AMPS, which is an analog cell phone, D-AMPS, which is pulsed with a pulse length of 6 miliseconds, and CDMA, which is digital but not pulsed. Use of cell phones was found to diminish the incidence of brain cancer in two studies conducted in the US between 1994 and 1998 [38] [58]. This result is be due to one or both of the following mechanisms:

(i) an auto-immune effect pursuant to the inhibitory (INH) effect as shown in Table "INH+ENS" column E on Figure 8. The increased power density during call-time caused the thymus to produce abnormally aggressive T-cells which had an anti-cancer effect when the phone user was un-exposed, resulting in diminished incidence of brain cancer in mobile phone users.

(ii) an auto-immune effect due to the temporary inactivation (INA) of T cells during negative selection causing a significant pro-auto-immune effect as shown in Table "INA+EPS+ENS" column R of Figure 8, also resulting in an anti-cancer effect.

The "Interphone" international study in which GSM was the dominant standard to which subjects were exposed [39] also confirmed that "moderate" GSM phone users also had a diminished brain cancer incidence as compared to non regular users.

[39] suggests that the strongest decrease could be for users having a cumulative call time below 5 hours during the 1 to 4 years before reference date because these users have an Odds Ratio of 0.68 with 95% confidence interval of 0.5-0.93 which is both significant and lower than most figures concerning more intense use. This is further confirmed by the fact that in a North European sub-study of Interphone the odds ratio of glioma in relation to ever use of a mobile phone was 0.63 (never users being the reference group) whilst it was only 0.78 for regular use (never users and non regular users being the reference group) [45]. It is further confirmed by a lower (though not significant) incidence of brain cancer for low latencies in [72] [40]. This may be due to the following reasons:

(a) a relatively minimal exposure time may be sufficient to maximize the anti-cancer effect (whether per Table "INH+ENS" or "INA+EPS+ENS") by generating any aggressive T cells which can reasonably be generated by exposure, after which further exposure does not improve the situation. This explains why more frequent exposures do not further decrease the incidence of brain cancer.

(b) the anti-cancer effect may be stronger when exposure is infrequent because otherwise regulatory mechanisms grow (section 2.6.1) and partly compensate the anti-cancer effect. Such mechanisms are likely to diminish the anti-cancer effect for "normal" users as compared to "very moderate" or very recent users.

The fact that "very moderate" or very recent users may have an abnormally diminished probability of being diagnosed with brain cancer makes overall results of such studies extremely sensitive to the choice of the reference group. The inclusion in the reference group of users having up to 39 hours cumulative call time is probably the underlying cause of the finding of a generally increased incidence of brain cancer in mobile phone users in [32].

The generally diminished incidence of brain cancer in moderate mobile phone users is further confirmed in [72] where it is found that it was found that a cohort comprising both NMT and GSM users had a significantly reduced brain cancer risk after 10 years latency as compared to the general population. The reason why there was not a comparable reduction of brain cancer for shorter latencies in this study is probably because the reference group was the general population rather than non-users, and the general population was widely equipped with GSM at the end of the follow-up period.

3.1.6 Increase of incidence rate of brain cancer in heavy cell phone users

In [39] a significant increase of brain cancer incidence was found for short-term heavy users of mobile phones. In [32] a comparable increase is confirmed for users of both digital (GSM) and analog (NMT) mobile phones that have a high number of cumulative hours of exposure. The result in [39] is dominated by GSM users. In [32] in the case of analog cellular phone users it is also shown that there is a significant increase of brain cancer incidence for latencies superior to 20 years, the increase becoming even more significant after 25 years. Since the most ancient users also tend to have the largest cumulative hours of exposure, the increase in [32] for the case of analog phone users is most likely in relation with the time since first use, rather than the "intensity" of phone use. Therefore, increases for GSM and analog users seem to have different characteristics:

- for users of GSM phones, there is an increase of brain cancer incidence in relation to the intensity of phone use (i.e. hours per year).

- for users of analog phones there is an increase of brain cancer incidence in relation with the time since first use, which becomes significant only after about 20 to 25 years.

The following interpretation can be proposed for each of these increases:

long term increase of cancer incidence in users of analog cellular phones I consider an analog cellular phone user having a developing neoplasm when he is younger than 40. This analog phone user benefits from an anti-cancer effect of the analog cellular phone as per table "INH+ENS" or table "INA+EPS+ENS" in figure 8. Thus a line of T cells is generated which controls brain cancer, whilst in the same situation a non-user of analog phone would immediately have developed brain cancer and probably died. This does not necessarily eliminate the neoplasm: the neoplasm may survive, and the T cell line keeps controlling it so that the neoplasm does not reach a detectable size. 25 years later, the T cell line in question may reach the end of its lifespan or have a reduced reproduction rate, or the nature of the cancer and the antigens presented by cancerous cells may have changed, so that the neoplasm gets out of control. The patient is most likely aged more than 60. His immune system is generally weaker than at a younger age. He is unable to produce a new line of T cells able to control the neoplasm again. He is thus diagnosed with brain cancer.

Thus, the cumulative increases of brain cancer for old patients who at a younger age were able to control their brain cancer only due to the anticancer effect of analog phones may be the underlying cause for the statistically observable increase of the cancer death rate for latencies of more than 20 years in [32]. This increase would thus be the counterpart of an earlier decrease.

short term increase of incidence in heavy users of GSM phones The pro-cancer effect of intense GSM use (in terms of brain cancer) is short term and is therefore unrelated to any exhaustion of a previous anti-cancer effect. It is further unrelated to any direct effect as per Table "INH+ENS" of Figure 8 which does not predict such a pro-cancer effect.

This pro-cancer effect is most likely due to the temporary inactivation effect (INA) causing a pro-cancer effect as per Table "INA+EPS" and "INA+EPS+ENS" for frequent high-power exposures. Near the handset, instantaneous power density of GSM pulses can reach roughly 80 W/m2, comparable to the instantaneous power densities which resulted in increased cancer growth in [78] and [66], discussed in section 3.1.1. The pro-cancer effects occurs for users having more than 1 hour/day of phone use, which is also comparable to the experimental exposures in [78] and [66]. This pro-cancer effect is thus essentially the same as discussed in section 3.1.1. This effect increases with power density as discussed in section 3.1.1, which would explain the laterality of the effect.

This pro-cancer effect depends on instantaneous power density rather than average power density because the mechanism (NRE) is dependent on the instantaneous power density. This explains why the effect was first noticed in GSM users, because analog cellular phones tend to have comparable average power density but lower instantaneous power density. However the same pro-cancer effect may affect analog phone users, although more marginally.

The pro-cancer effect as per Table "INA+EPS" and Table "INA+EPS+ENS" column F competes with the anti-cancer effects as per Table "INH+ENS" and Table "INA+EPS+ENS" column R, but becomes dominant for brain cancer over about 1 hour of daily phone use. Since the power density and exposure range for the effect are within the range of Table "INH+ENS" corresponding to the experimental findings in [78] it is unlikely that abrupt interruption of GSM use would cause a strong pro-autoimmune effect as shown in Table "INA+EPS+ENS" column R, and the pro-cancer effect is expected to last for quite long after termination of GSM use as is the case in [78], because it essentially results from elimination of a significant number of T cells by positive selection (EPS).

3.1.7 Temporary increase of cancer incidence near cell phone base stations

Exposure to a GSM base station differs very notably from exposure to an individual GSM phone. Residents living near a GSM base station are exposed full-time rather than part-time. In the hypothetical case of a permanently overloaded GSM base stations permanently using all available frequency sub-carriers and all available time slots, the signal transmitted by such base station is quite similar to a gaussian signal having a constant envelope and therefore when this hypothetical overloaded base station is turned on for the first time, residents living nearby are submitted to a pro-cancer effect due to the low to high transition as per Table "INH+ENS" column C on Figure 8.

In practical cases the load of a base station is variable. At start-up of the base station (or following an increase of traffic) some T cell lines which previously controlled cancer suddenly become unable to bind their corresponding pMHC, so that the transient pro-cancer effect dominates. On the longer term the transient pro-cancer effect disappears and a long term anti-cancer effect may dominate.

In [87] the incidence of cancer cases near a cell phone base station was studied from 1 year after the onset of the cell phone base station to 2 years after the onset. The cell phone base station came into service in 7/96 and was GSM or GSM-like. Cancer incidence was abnormally high as compared to both a nearby area and the general population. 7 out of 8 cancer victims near the cell phone base station were women. It is not specified whether victims recovered or died. The power density to which the local residents were submitted was $5.3 \cdot 10^{-3}$ W/m2. The residents were initially submitted to a pro-cancer effect due to the constant background power density emitted by the GSM base station. T cells which were controlling cancer lost control at the onset of the GSM base station due to the transition to the constant GSM background, causing the observed high number of cancer cases one year after the base station was turned on.

Replacement of these T cells by other lines of T cells may have been speeded up by the permanent anti-cancer effect owed to the time variations of the GSM signal (i.e. day/night variations, for example). However it was insufficient to avoid cancer in the specific case described in [87].

In [87] most cancer victims were women. This is somewhat surprising in view of the fact that in Paris in 2005 the reaction to DVB onset was stronger in men (see section 3.1.9). [87] does not give any indication as to the professional occupations of victims, but a potential explanation for the unusual sex ratio may be a higher number of non-working women or of women working and living in the same exposed area, as compared to the number of non-working men or men working and living in the exposed area. Persons who work outside the exposed area have a part time low exposure during which the immune response remains efficient, which brings their case towards Table "INH+EPS" column E corresponding to an anti-cancer effect. This explanation would not hold if the (INA) effect was dominantly implied, because the (INA) effects lasts more than 12 hours and would thus cause roughly the same pro-cancer effects on persons submitted temporarily or permanently to exposure. As the applied power od $5.3 \cdot 10^{-3}$ W/m2 is the highest power at which strictly (INH) effects were found, this order of magnitude was used as the limit of typical powers for the (INH) effect in Figure 8.

3.1.8 Increase in cancer incidence near TV emitters

In [18] and [19] leukemia incidence near 21 high power radio and TV transmitters in the United Kingdom was examined. The study concentrated on the difference between cases in the 0-2 km range around a transmitter and cases in the 0-10 km range, however published results also comprised the number of leukemia cases in the 0-10 km range around the emitter as compared to the average UK number of leukemia cases (adjusted regionally and by age, sex, year and deprivation quintile). 3 emitters had a significantly higher number of leukemia cases in the 0-10 km range around the emitter than the average UK number of leukemia cases. One emitter had a significantly higher number of leukemia cases in the 0-2 km range but not in the 0-10 km range. No emitter had a significantly lower number of leukemia cases than UK average.

Ranking the emitters by expected number of leukemia cases in the 0-10 km range, the three emitters having the largest numbers of expected cases in each case had significantly higher numbers of leukemia cases than UK average either in the 0-10 km range (Crystal Palace, Winter Hill) or in the 0-2 km range (Sutton Coldfield). Averaging on all sites that had a TV emitter above 500 kW also yields a significantly higher number of leukemia cases than UK average.

Only in Sutton Coldfield was the total number of cancer cases compared with UK average, and it was significantly higher than UK average both in the 0-2 km range and in the 0-10 km range. This is a clear indication that not only leukemia, but also the all-cancers incidence was abnormally high near TV emitters.

The study covered all leukemia cases between 1974 and 1986, i.e. a 12-year period. In Sutton Coldfield the observed/expected ratios for all cancers was 1.03 in the 0-10 km range with the 95% confidence interval being 1.02 to 1.05. For leukemia, in all places individually the average observed/expected ratio of 1.05 was within the confidence interval. So the increase in cancer incidence was limited, despite being significant. Taking a 5 % increase as an hypothetical value of the real increase (observed/expected=1.05), if in fact observed it would have been expected to yield significant results only in Sutton Coldfield for "all cancers" , in Crystal Palace and in averaged figures for "all leukemias". In all cases it was actually observed. Other individual places or Sutton Coldfield for "all leukemias" could generally not yield individually significant figures by lack of a sufficient population. Where significant figures were obtained, the observed/expected value was much above the 5 % limit. This explains why most individual places in the study did not yield significant increases for all leukemias.

In the present model the effect of a low power density exposure to a TV signal, which has a large bandwidth and relatively limited time variations, is expected to be ruled essentially by Table "INH+EPS" column C in Figure 8, i.e. the increase in cancer incidence would be expected to occur essentially temporarily, following increases in power and/or bandwidth of the emitters. The increases of cancer incidence observed on a 12-year period may result from temporary increases having occurred during the period. For example in Sutton Coldfield the number of frequencies on which TV was being broadcast at 1 MW equivalent power rose from 3 to 4 frequencies in 1982, causing a transient pro-cancer effect.

3.1.9 Temporary increase of cancer death rates after onset of DVB emitters

In [18] and [19] the increases in cancer incidence were limited. However, if they result at least in part from temporary increases occurring within a global timespan of 12 years, single increases within this timespan may be higher and more easily observable than the averaged increase.

In order to test the hypothesis that transient cancer

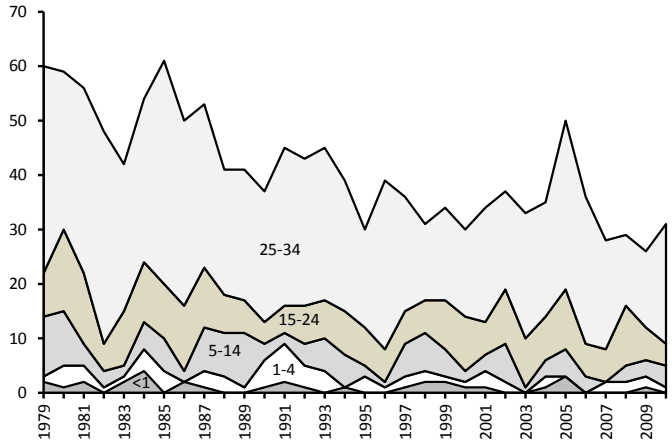

Figure 10: number of deaths due to neoplasms in Paris for men in younger age groups

	All < 34		All 25-34		Men 25-34		Women 25-34	
	Numb.	P+	*Numb.*	P+	*Numb.*	P+	*Numb.*	P+
1985	108	0,121	71	0,051	41	0,051	30	0,241
1986	83	0,995	56	0,971	34	0,971	22	0,946
1987	83	0,913	49	0,974	30	0,974	19	0,935
1988	87	0,730	52	0,825	23	0,825	29	0,206
1989	77	0,944	49	0,871	24	0,871	25	0,796
1990	70	0,984	44	0,949	24	0,949	20	0,931
1991	73	0,910	47	0,830	29	0,830	18	0,932
1992	67	0,921	41	0,903	27	0,903	14	0,983
1993	79	0,388	52	0,251	28	0,251	24	0,299
1994	74	0,728	50	0,628	24	0,628	26	0,368
1995	54	0,997	38	0,975	18	0,975	20	0,903
1996	78	0,168	59	**0,046**	31	0,046	28	0,192
1997	61	0,980	42	0,992	21	0,992	21	0,927
1998	62	0,831	37	0,980	14	0,980	23	0,646
1999	62	0,783	34	0,975	17	0,975	17	0,944
2000	53	0,953	31	0,979	16	0,979	15	0,961
2001	59	0,718	36	0,786	21	0,786	15	0,923
2002	68	0,259	35	0,799	18	0,799	17	0,768
2003	55	0,953	33	0,705	23	0,705	10	0,985
2004	65	0,344	38	0,308	21	0,308	17	0,451
2005	86	**0,007**	56	**0,004**	31	**0,004**	25	**0,041**
2006	50	1,000	36	0,998	27	0,998	9	1,000
2007	53	0,974	34	0,972	20	0,972	14	0,799
2008	55	0,872	29	0,986	13	0,986	16	0,558
2009	57	0,746	34	0,798	14	0,798	20	0,202
2010	49	0,949	31	0,886	22	0,886	9	0,998

Table 8: yearly number of cancer deaths and calculated P+ for various age and sex groups in Paris. Significant increases (P+<0.05) are in bold and underlined.

increases do appear after onset of TV emitters, I used the yearly statistics on causes of death [11] for the years prior to and after the first installation of DVB emitters, in march 2005 in Paris. In march 2005, 5 DVB channels of 8 MHz each started emitting, resulting in a sudden increase of emitted power and - most importantly - bandwidth and an expected transient pro-cancer effect. For reference, the power of the Eiffel tower emitters was 20 kW on each of the 5 new channels (as compared to 500kW to 1000 kW per channel in [18] [19], and as compared to 100 to 200 kW per channel on the pre-existing analog emitters of the Eiffel tower).

This pro-cancer effect is indeed evidenced by figure 10 which shows a marked increase of cancer death rate in men aged less than 34 for the year 2005 corresponding to the first 9 months after DVB onset.

The statistical significance of the increase of cancer death rate in Paris for the years 1985 to 2010 was evaluated using the procedure described in Appendix C for various age and sex groups (table 8). The increase is most significant for men aged 25-34 yet cancer death rate increased significantly in each of these groups.

This increase is in full agreement with the hypothesis. The most affected category was men aged 25-34. This can be interpreted as follows: in younger age classes thymus output is higher and the transition period was too short to allow a significant increase of cancer death rate. Further, in men aged 35-44, cancer death rate increased significantly in 2006 only (not shown), showing the effect of a further increase of the transition period due to further thymus involution and of generally slower cancers in this age category. Further age categories were not significantly affected.

A survey of the about 3047 official field measurements individually reported in [2] and made in Paris between march 3, 2011 and december 11, 2012 (after the shutdown of the analog emitters but before the onset of further DVB emitters) shows that in 99% of cases the maximal power density on any single DVB multiplex was below $2 \cdot 10^{-6}$ W/m2 and that the maximal integrated TV power density ever measured during that period was 10^{-3} W/m2, with an average power density of $6 \cdot 10^{-5}$ W/m2 amongst the 1% of measurements yielding more than $2 \cdot 10^{-5}$ W/m2 on a single multiplex. On the balance of probabilities it is thus overwhelmingly likely that the observed temporary increase of cancer death rate was caused by a DVB power density of less than $2 \cdot 10^{-6}$ W/m2.

3.1.10 Increase of melanoma incidence with the number of FM transmitters

In [31] it is shown that melanoma incidence in Sweden increases with the number of covering FM radio transmitters and it is proposed that FM radio emissions may be a non-negligible contributor to the increase of melanoma incidence. This raises the question of whether melanoma may behave differently as compared to other cancers, and react to a relatively low power density exposure by a permanent - rather than temporary - increase in incidence.

In the low-frequency domain (wavelength >> human body dimensions) the electric field is essentially equilibrated by superficial charges on the surface of the human body. The electric field inside the body is very strongly attenuated, and there is essentially a field discontinuity on the surface of the skin, with a higher field outside the body than inside. In the high-frequency domain a wave has a penetration depth. It is attenuated, but less strongly. The FM range, with a wavelength of the same order of magnitude as the size of the human body, is intermediate between these situations.

Generally, the electric field is thus expected to be stronger on the skin surface than inside the human body. Therefore, T cells are thymus - selected with an electric field (inside the thymus) which is lower than the electric field on the skin. T cells which survive thymus selec-

tion are adapted to recognize cancerous cells inside the body, and their ability to recognize cancerous cells is diminished on the skin due to a higher electric field having an inhibitory effect (INH) relative to the lower field in the thymus (which sets the selection criteria for T cells). Therefore the incidence of melanoma may be permanently increased by a permanent low-power electric field, which is not the case of the "average" cancer.

Thus, the proposal that melanoma incidence would permanently increase with permanent exposure (and more particularly FM radio exposure), although an exception to the general findings in Table "INH+ENS" of Figure 8, is in agreement with the present model.

3.1.11 The "multiple waves oscillator"

A device described in [46] [69] was used successfully to cure cancer in the 1930s [63] [47]. This device essentially emits a broadband signal. The patients were typically exposed 15 minutes, the exposure being repeated a few times at intervals of a few days. Exposure bandwidth was high, superior to 3 GHz, possibly affecting most T cells, which explains the high reported efficiency of the system. Power density for exposure is unknown.

The Lakhovsky multiple waves oscillator (MWO) probably acted through a mix of the inhibitory effect (INH), and of the inactivatory effect (INA), acting both on the tumor and on the thymus. A proposed explanation of how it worked is based on the following three mechanisms:

(i) The inhibitory effect (INH) combined with thymus negative selection (ENS) generates an anticancer effect pursuant to Table "INH+ENS" column E in figure 8.

(ii) The inactivatory effect (INA) combined with thymus selection generates an anticancer effect pursuant to Table "INA+EPS+ENS" column R in figure 8.

(iii) When a cancer develops, it changes [37], and the presented antigens also change. A line of T cells which was originally efficient in fighting the cancer may become less efficient. In such cases, the tumor may comprise cancerous cells and T cells of an original line which have a low (though existent) capacity to recognize the cancerous cells, which are unable to enter the temporarily inactivated state (TI), and therefore block or reduce accessibility of the tumor for other T cell lines. The Lakhovsky field may temporarily inactivate the original line of T cells. Temporary inactivation of the original line yields evacuation of the original line from the tumor area, which becomes accessible to other T cells. This allows other T cells, which may be more efficient against the tumour, to access cancerous cells in sufficient numbers and to get cloned and replace the original line. The original line of T cells is thus replaced by a new line of T cells which may be derived from a pre-existing mature T cell, possibly from a pre-existing line of T cells which was already active against the tumor but unable to access the bulk of the tumor. So the anti-cancer effect in this case may be independent of thymus selection. It may also depend on thymus selection if the original line of T cells is replaced by a recent thymic emigrant.

The respective share of effects (i) (ii) (iii) is difficult to determine and may have varied from patient to patient. In some cases immediate effects of exposure were observed, which is most likely attributable to effect (iii) yielding an immediate change in the tumor. On the other hand, treatment typically lasted a few weeks, which is about the thymus transit time, corresponding to the need for T cells having escaped steps of thymus selection to transit through the thymus and reach the tumor. It is likely that effects (ii) and (iii), which are expected to occur in about the same conditions, were both implied. Assuming the power density was adapted to have effects (ii) and (iii) dominate, the contribution of effect (i) may have been less essential.

3.1.12 Transition between tables "INA+EPS" and "INA+EPS+ENS"

In [78] the exposure of mice during 1 month at 100 W/m2 2 hours daily 6 days a week resulted in a pro-cancer effect after the end of the exposure month. In [29] exposure of rats during 1 month at 5 W/m2 7 hours daily 5 days a week resulted in a pro-auto-immune effect after the end of the exposure month. This difference is due to different exposure power densities causing the (INA) effect to be either pro-auto-immune or pro-cancer as discussed in section 2.4.4. This difference is also the essential difference between tables "INA+EPS+ENS" and "INA+EPS" in Figure 8.

Likewise, in [39] the fact that the anti-cancer effect dominates at low exposure time and the pro-cancer effect dominates at high exposure times is related to both the competition between the (INH) and (INA) mechanisms and to the shift of the (INA) mechanism from being pro-auto-immune for rare exposures (Table "INA+EPS+ENS")to pro-cancer for high daily exposures (Table "INA+EPS") as discussed in section 2.4.4.

3.2 Effects of electromagnetic waves above 9 GHz

3.2.1 Effect of millimeter wave irradiation on tumor necrosis factor production

In [24] mice were continuously irradiated with cw millimeter waves at 10 GHz. The production of TNF (Tumor Necrosis Factor) by T cells was higher for the irradiated mice than in the control group during the first 24 hours of exposure time, but not after 72 hours.

This can be interpreted as follows:

(a) the irradiation at 10 GHz had a stimulatory effect (ST) on TCR-pMHC recognition as discussed in section 2.2.4.

(b) during the initial period this stimulatory effect directly resulted in an increased aggressiveness of T cells yielding increased production of TNF.

(c) simultaneously, in the thymus the stimulatory effect on TCR-pMHC recognition resulted in elimination of more T cells by negative selection.

(d) most likely, the decrease of TNF production after 72 hours is due to both the reduced aggressiveness and numbers of recent thymic emigrants attributable to the increased negative selection in the thymus, and to the elimination of older T cells having become abnormally aggres-

sive under exposed conditions, by extra-thymic regulation mechanisms. The 72 hours duration is consistent with the short thymus transit times in mice, possibly in the order of 2 days [82].

Basically, a transient anti-cancer effect as per Table "ST+ENS" column C on figure 8 is observed.

3.2.2 Effects of the Priore system on pathogens

In [4] mice were infested with trypanosoma equiperdum, then exposed 6 continuous hours/day during 3 days in a complex apparatus [64] to a pulsed wave at 9.4 GHz, amplitude modulated at 17 MHz, and simultaneously to a slowly modulated magnetic field at 1 kGs. The evolution of parasitemia was monitored as a function of time and of the power of the 9.4 GHz wave. In non-exposed controls parasitemia increased continuously until death. In sufficiently exposed animals parasitemia decreased and animals survived. The decrease of parasitemia was faster when animals were exposed to a higher power.

However, when animals were exposed to the 9.4 GHz wave non-modulated and without the magnetic field (but pulsed), there was no significant effect and infected animals died. Thus, even if the 9.4 GHz pulsed wave possibly had a stimulatory effect on immunity, it was insufficient per se to obtain the observed effect and it was heavily enhanced by either or both of the modulation or the magnetic field.

These findings are in agreement with an effect based on the stimulation effect at a power density sufficient to reverse the $\Omega_c << \Omega_b$ condition (STM in Figure 8). As discussed in section 2.2.4 if the power density of the 9.4 GHz wave is strong enough to reverse the $\Omega_c << \Omega_b$ condition, the likelihood of the (a) to (c) transition becomes low and the wave must be amplitude modulated (as discussed in section 2.2.5) to render such transitions possible. Although the pulsed nature of the wave already provides some level of modulation, the much faster 17 MHz amplitude is likely to have been much more efficient in this respect, which explains the need for this modulation.

The slowly varying magnetic field was costly to produce and was probably there for a good reason. The difficulty with stimulating the (b) to (c) transition with a cw wave is that transitions can occur only between quantum states which have an energy difference corresponding almost exactly to the frequency of the cw wave. Otherwise the cw wave does not affect the system. The magnetic field may have alleviated this requirement by:

(i)splitting degenerate energy levels in wells (b) and/or (c) by Zeeman effect. Degenerate energy levels in well (b) may arise because the one-dimensional picture used in part 2.2 must be replaced, for better correspondence with the real world, by a multi-dimensional picture corresponding to the many degrees of liberty in biological molecules. For example, the combination of energy levels of well (b) with independent translational or rotational energy levels is expected to yield degenerate energy levels. This increase in the number of available quantum state energies in each quantum well is expected to increase the number of transitions which can be stimulated with a single cw wave and could explain why the magnetic field was necessary or at least useful.

(ii) varying the energy of each energy level (whether such energy level is split or not) in a time-dependent manner, so that the difference between energy levels will correspond to the frequency of the cw wave at least part-time. The effect of such variation of the energy of each energy level is in essence comparable to the effect of varying the frequency of the cw wave over time, which was shown in [24] to improve the immune-stimulatory effect.

Another remarkable fact is that the discussion in section 2.2.5 predicts a variation of the effect with the power density of the applied wave, which was not observed. This lack of variation of the effect with the power density of the applied wave is likely related with the presence of the slowly varying magnetic field, which changes the frequencies of the quantum states over time. This is expected to also modify the Rabi frequencies of transitions between wells, and thus to modify the power density needed for a maximal immune-stimulatory effect, so that the effect will vary over time from immune-stimulatory to neutral or even inhibitory (based on section 3.2.4 the effect may also be inhibitory). Generally, if system efficiency changes over time, the overall efficiency against the pathogen tends to be determined by the most favourable conditions because a short period of high immune efficiency can compensate long periods of lack of efficiency. So, variations due to the slowly changing magnetic field can be expected to result in an overall anti-pathogen effect without significant power density-dependent variations of the effect.

In short, it is highly likely that the "Priore" system did work on the basis of the stimulatory effect (STM) with the 17 MHz modulation being necessary to allow stimulated transitions from (a) to (b) and with the magnetic field acting to reduce the bandwidth requirements by splitting degenerate levels and modifying energy levels in a time-dependent manner.

3.2.3 Effects of the Priore system on cancer

In [67] the effects of the Priore system on cancer were observed. Exposure of cancerous rats for up to 90 mn daily resulted in tumour regression. This is in agreement with the discussion in section 2.2.4 : for short exposures the effect of thymus selection can essentially be ignored, and the overall effect is dominated by the increase of aggressiveness of normally selected T cells, yielding an anti-cancer effect as per table "ST+ENS" column E (based of (STM) in the present case). The longer exposures were more efficient because there was more time available for T cells in an abnormally aggressive state to attack cancerous cells.

3.2.4 Effect of amplitude-modulated pulsed wave on antibody response

In [84] mice were exposed 10h per day for 5 days in a Faraday cage to a 9.4 GHz pulsed wave with pulse length $1\mu s$ amplitude modulated at frequencies in the range of 14 to 41 MHz or non-modulated, with peak instantaneous power density of 300 W/m2. When not exposed, the mice were not in the Faraday cage. There was also a non-exposed control group, which never entered the Faraday cage. The antibody response to immunization was assessed.

It was found that the antibody response was either diminished or increased by exposure (with respect to the control group) depending on modulation frequency, with a plurality of maximums and minimums.

This experimentation can be interpreted as follows:

During the 10-hrs exposure periods, the exposed mice were subject to an immuno-stimulatory effect due to the modulated wave, with frequency-dependent maximums as discussed in section 2.2.5. At least qualitatively, this immuno-stimulatory effect explains the frequency-dependent maximums of antibody response which were observed. However the fact that the antibody response at its minimums was lower than in the control group, is less easily explainable within the simple mathematical model used herein. A more elaborate model will thus be necessary to account for it.

The fact that in this experimentation maximums and minimums of the antibody response were little dependent of the specific antibody being examined is of some importance. As appears in section 2.2.5 the maximums depend only on the Rabi frequency Ω_{cart} of transitions stimulated by the artificial wave. At fixed power density and frequency, they depend only on the overlap $O_{b;c}$ between the quantum states $|b\rangle$ and $|c\rangle$ as defined in Appendix A. The fact that maximums and minimums do not vary with the choice of the antibody essentially shows that the overlap $O_{b;c}$ is independent on the T cell and antigen, and in particular does not vary with the hyper-variable part of the T cell. Therefore, the (b) to (c) barrier would be an essentially stable structure identically reproduced in all T cells of the same organism and probably of the same lineage of mice, which differs from the (a) to (b) barrier which is expected to vary between different T cells and be modified by the presence or absence of the antigen.

3.3 Hyperthermia

The detailed analysis in 2.3 implies that fever stimulates the TCR-pMHC recognition. Mild hyperthermia can be viewed as an artificial fever, so that the conclusions concerning fever also apply to mild hyperthermia.

In [54] and [75] it is confirmed that mild hyperthermia enhances T cell cytotoxicity. This is in full agreement with the proposed model. In [54] hyperthermia is performed prior to the cytotoxicity test in a 6-hours long incubation phase. The hyperthermia effect on cytotoxicity appears as a delayed, non-instantaneous effect. A proposed interpretation is that quantum well (a) would only have a "weak" link to a thermostat, so that the increase in temperature results in a change in the occupation of quantum well (a) but only after a sufficient time, and more importantly the occupied levels in quantum well (a) would not become un-occupied instantaneously after a drop in temperature. This would also be consistent with considering well (a) as essentially isolated from anything else than well (b) during the interaction.

In [68] it is shown that whole-body hyperthermia (2h daily for 7 days starting day 14 after tumor inoculation) caused temporary regression of a tumor and at the same time resulted in an elevation in the number of ling metastases in mice. This is attributable to the influence of the hyperthermia session on thymus selection. During the hyperthermia session, the TCR-pMHC recognition is stimulated in the thymus, resulting in a stronger thymus selection. Cells which are produced by the thymus during the hyperthermia session are less efficient against cancer than cells normally produced by the thymus. The hyperthermia session thus results in a delayed pro-cancer effect.

In [68] normal animals exposed to hyperthermia prior to implantation of neoplastic cells exhibited significantly accelerated tumor growth and an increased number of spontaneous metastases as compared to controls. This is also attributable to the effects of hyperthermia on thymus selection: the T cells produced by the thymus during the session were less efficient against cancer than they would otherwise have been. When later exposed to a cancer, they were less efficient in controlling it than the C cells of control animals.

In [17] rabbits were exposed to hyperthermia 1h/day for 3 days starting on day 35 after tumor inoculation, at 42 deg intra-tumor temperature. Tumor regression (on up to 14 weeks) was much faster on rabbits having undergone local hyperthermia than on rabbits having undergone whole-body hyperthermia. Also in this case the effect of hyperthermia on thymus selection mitigated its direct effects on the tumor. Interestingly, the rate of change of tumor volume did not significantly differ between local and whole-body hyperthermia during the first two weeks after start of hyperthermia, and serious divergence appears only from week 3 onward, reflecting typical thymus transit times which are in the order of 2 weeks [55]

In [53] it is reported that murine T cells exposed to hyperthermia at 43 deg were inhibited rather than stimulated. Although slightly surprising in view of the above discussion, this result could possibly be explained as described in section 2.3.3.

4 Overview and proposed experimentations

4.1 Overview of discussed references

The model in itself shows which effects are favoured by certain characteristics of artificial waves, but it does not set precise boundaries between different effects. The boundaries indicated on Figure 8 are therefore deduced from the experimental data summarized on tables 9 and 10.

4.2 What can be confirmed ?

The outcome of any particular experiment is determined by the frequency, power density and bandwidth of the artificial electromagnetic wave. However, because the phenomenons were not understood, the experiments did not yield the best results and unintended environmental exposure interfered with a number of experiences, strongly influencing the outcome.

Generally, it is proposed to realize experimentations aimed at testing aspects of the model "one by one", and avoid any mix of various effects, so as to obtain results which are as easily interpretable as possible. It is of particular importance to control environmental artificial waves

effect	disease	col	reference	freq	instant. power density	bandwidth, duration
INA	(in vitro)		Lyle et al. [52]	450 MHz	15 W/m2	60 Hz
INH+ENS	cancer	E	Wolf and Wolf [87]	900 MHz	0.005 W/m2	60 MHz
			(a)	450-780 MHz	10^{-6} W/m2	40 MHz
		(b)	Hallberg and Johansson [31]	100 MHz	?	0.05-1 MHz
INA+EPS+ENS	autoimmunity	R	Grigoriev et al. [29]	2.4 GHz	5 W/m2	cw 7h/day 30 days
			Vinogradov and Dumanski [85]	2.4 GHz	0.5 W/m2	cw 5h/day, 14 days
	$\simeq$ infection(g)	F	Dronov and Kiritseva [20]	UHF	0.5 W/m2	cw 4 h/day 4 months
INH+ENS INA+ENS+EPS	cancer	E,R	Lakhovsky [47]	0-3GHz	?	3 GHz 15 mn 3 times
INA+EPS	cancer	B	Szudinski et al. [78]	2.4 GHz	50-150 W/m2	cw 2h/day 1-6 months
INA+ENS+EPS INA+EPS	cancer	B	Repacholi et al. [66]	900 MHz	20-100 W/m2	2kHz,1h/day
	dev.tim.(f)	B	Bornhausen et al. [7]	2 GHz	29W/m2	5 MHz 22h/day
		B	Bornhausen et al. [7]	900 MHz	28W/m2	200 kHz 22h/day
		B	Takahashi et al. [79]	CDMA		20h/day
ST+ENS	cancer	C	Fesenko et al. [24]	10 GHz	0.01 W/m2	cw
STM+ENS	cancer	E	Riviere et al. [67]	9.4 GHz	?	pul,am,M,10-90 mn/day
	infection	E	Berteaud et al. [4]	9.4 GHz	?	pul,am,M,max 70 h
	$\simeq$ infection(g)	E	Veyret et al. [84]	9.4 GHz	300 W/m2	puls,am 10h/day,5 days
FEV	(in vitro)		Mace et al. [54]			
			Smith et al. [75]			
	cancer	(d)	Dickson and Muckle [17]			
		(e)	Roszkowski et al. [68]			

Table 9: experimental results essentially attributable to a single effect or to a plurality of effects having the same outcome. (a) data from [11], see section 3.1.9. (b): exception to the predictions of column B, see section 3.1.10. am: amplitude modulated. M: presence of a slowly varying magnetic field. (d) local vs whole-body exposure (e) short term vs long term effect of whole-body exposure. (f) disturbances of developmental timing parameters, see text for details. (g) reaction to sensitization with non-self antigen. pul: pulsed. am: amplitude modulated. Column numbers (col) and effects refer to Figure 8.

dominant effect	competing effect	reference	instantaneous power density, bandwidth,duration
INH+ENS (E) INA+ENS+EPS(R)	INA+ENS+EPS (F) INA+EPS (E)	Interphone [39](b) Schuz et al. [72] Hardell et al. [32](a)(b)	< 80 W/m2,200 kHz,<1h/day
		Muscat et al. [58](c) Inskip et al. [38](c)	
INA+ENS+EPS (F) INA+EPS (E)	INH+ENS (E) INA+ENS+EPS(R)	Interphone [39](b) Hardell et al. [32](b)	<80 W/m2,200kHz,>1h/day
INH+ENS (C, D)	INA+ENS+EPS(R)	de Gannes et al. [16](d)	
INA+ENS+EPS (F) INA+EPS (E)	INH+ENS(D)	Buschmann [9](d) Buschmann [10](d) Lerchl [50](d)	

Table 10: experimental results below 3 GHz attributable to competition between different effects. (a) effects in this reference are dominantly anti-cancer for moderate users despite being apparently pro-cancer, see text for details. (b) The same statistical results are dominated by different effects, depending of exposure time. Only GSM modulation parameters are shown but analog systems were also used. (c) mix of AMPS, D-AMPS and CDMA. (d) neither of the competing effects is fully dominant and the (INH) effects are due to unintentional environmental exposure. Column numbers (col) and effects refer to Figure 8.

in each experimentation. The model has many different aspects which can be tested based on this general principle.

The most essential practical aspect of the model is that provided a certain bandwidth threshold is exceeded, the inhibitory effect (INH) may take place and cause verifiable disturbances of the human immune system at extremely low power density, well within the range to which human populations are submitted. This aspect of the model is statistically confirmed in [87] at 0.005 W/m2 and in the variations of cancer death rates at DVB onset in Paris, at a power density which is most likely below $2 \cdot 10^{-6}$ W/m2 (section 3.1.9). It is also a major explanatory factor, after re-interpretation of the results, in [16], [9], [10].

However this aspect of the present model has never been intentionally tested "per se" in vitro or even in an animal model. The usual considerations that coincidence is not causation are likely to be opposed to the statistical verifications in this case. Most importantly, this aspect of the model has far-reaching practical implications, so that a high standard of proof is likely to be required. It would thus be particularly interesting to make direct and intentional tests of this aspect of the model, both in vitro and in vivo. The next sections will essentially concentrate on these proposed confirmations.

An ancillary aspect which would require confirmation is the variations of developmental timing predicted by the reasoning in section 2.6.6. These variations have been observed only in the case of high permanent exposure, and are linked with near certainty with the lack of immunity observed in these cases. However the link between immunity and developmental timing is not a generally recognized fact and predicted variations applying for Table "INH+ENS" are based on a reasoning which is somewhat isolated from the remainder of the model. It would thus also be important to verify this link experimentally.

4.3 Proposed in vitro confirmation of the effects of low-power large-bandwidth radio-frequency waves

Methods for in vitro testing of cytotoxicity are known [52] [8]. These methods can be applied for testing cytotoxicity variations upon exposure to low power density artificial waves. The cytotoxicity test must be made in exposed conditions (rather than after exposure) because unlike the effect of temporary inhibition (INA), the inhibition effect (INH) is not expected to last after the end of exposure.

Although figure 8 shows possible interactions between a number of effects, using a power density below $5 \cdot 10^{-3}$ W/m2 (order of magnitude of exposure in [87]) and frequencies between roughly 100 MHz and 3 GHz is generally expected to ensure that the sole mechanism implied is the inhibitory effect (INH), and to exclude the inactivatory effect (INA, which was never found to exist below 0.5 W/m2), and the stimulatory effect (ST, STM) which takes place above 9 GHz. Thus, the inhibitory effect (INH) can be easily isolated from other effects of electromagnetic waves.

Some preliminary assays may be necessary to find a suitable electromagnetic wave. In view of the observations in section 3.1.9 and 3.1.7, a typical electromagnetic wave could be any wave within the 500 MHz- 1 GHz range having a bandwidth of about 70 MHz (the order of magnitude of the cumulative GSM or DVB bandwidth) and a power density somewhere between $2 \cdot 10^{-6}$ (order of magnitude of the DVB power density in Paris) and $5 \cdot 10^{-3}$ W/m2 (order of magnitude of exposure in [87]). However, the suitable electromagnetic wave depends on the specific T cell line being used since different T cell lines may have different frequency, bandwidth (Δ_b) and power conditions. Therefore, more than one try may be necessary to find a suitable wave for a specific T cell line. Alternatively, a large bandwidth in the order of 3 GHz can be used. In this case there is potentially a higher likelihood to obtain unexpected results due to the activation of any inhibitory receptors but on the other hand the efficiency of the Lakhovsky system [47] which has a bandwidth of about 3 GHz is a serious indication that in a majority of cases this does not happen.

In such an experience it is essential to use a suitable RF and animal breeding protocol. The experiments should generally be made in a Faraday cage having a sufficient attenuation of external wavelengths to attain "thermal level" inside the Faraday cage, i.e. the spectral power density inside the Faraday cage must be as given by Planck's law. The efficiency of the Faraday cage should be checked by appropriate measurements of the residual fields inside the cage. Also, it is not sufficient to use a Faraday cage during the "in vitro" stage of an experiment. If T cells are formed in an animal exposed to common environmental levels of exposure to artificial waves, the T cells when isolated and placed in a Faraday cage will undergo unpredictable variations of their binding capabilities (normally an increase of their binding capability). This can bias the whole experimentation. Therefore the animals themselves should be bred in Faraday cages, ideally for more than one generation - as was in essence done, although with unspecified efficiency of the Farady cages, in [76]. If it is desired to obtain a highly reproducible experience, MHC testing of the animals and/or using the same lineages in each parallel experiment can be useful precautions.

Once first results are obtained, varying experimental conditions should make it possible to find out the detailed bandwidth, frequency and power conditions that apply to any specific line of T cells.

4.4 Proposed in vivo confirmations of the effects of low-power large-bandwidth radio-frequency waves

The same observations concerning the RF and animal breeding protocol and the applicable power density or bandwidth apply in vivo as for in vitro experiments. Multi-generational studies could be used to test the effects of low-power large-bandwidth radio-frequency waves as per Table "INH+ENS" of Figure 8

To verify effects as per Table "INH+ENS" column E it is possible to inoculate the animals of the second generation with cancerous cells, and to monitor the evolution of cancer, which is expected to be overcome more easily in animals undergoing temporary exposures than in sham-exposed controls. In this case exposure times should be

limited, for example, to a few hours daily.

To verify permanent effects on pathogens, the limited daily exposure must be replaced by a permanent exposure to a white noise signal of appropriate bandwidth and power density, so as to provoke a permanent pro-pathogen effect. The animals of the second generation may be inoculated with a pathogen and the endpoints can be the viral or bacterial load or the parasitemia. Exposed animals are expected to have a delayed and/or weakened immune response.

To verify transient effects on cancer (or pathogens), the animals may be first left in a Faraday cage for one generation, then the second generation can be inoculated with cancer (or a pathogen), and simultaneously exposure can be started. Exposed animals are expected to develop cancer more easily.

It is also possible to verify the effects on an ongoing primary immune response. In this case, exposure is started after the start of a primary immune response following inoculation of cancer or pathogens. The endpoint would be the evolution of cancer, viral load or the like. Exposure is expected to interrupt a proportion of the ongoing immune responses and to delay start-up of replacement immune responses.

Other procedures can be easily designed to test other predictions of Table "INH+ENS".

The possible impact of low-power high-bandwidth electromagnetic waves on developmental timing, discussed in section 2.6.6, could similarly be verified by applying field variations corresponding to the different cases of table "INH+ENS" and observing developmental timing endpoints.

4.5 Proposed statistical confirmation of the effects of low-power large-bandwidth radio-frequency waves

Table "INH+ENS" of Figure 8 predicts different possible effects of electromagnetic waves on four generic classes of diseases. The conditions in which different diseases are affected may vary depending on the specific disease considered. Using cause of death statistics as correlated to changes in the electromagnetic environment could make it possible to observe whether the predictions of Table 1 are verified for other diseases than cancer. With respect to cancer, comparative studies between groups of cities having undergone similar changes in electromagnetic environment and groups of cities not having undergone such changes would be welcome to confirm the statistical results found for Paris.

Generally, statistical verifications must cope with a few difficulties. In particular, interaction between different sources of electromagnetic waves cannot be avoided and may yield to unexpected results. Comparisons between different places may be affected by such aspects, in addition to other geographical variations in diseases. Yet, statistical verifications would be fundamental both in confirming theoretical predictions and in assessing the impact of artificial electromagnetic waves on public health.

5 Conclusions

The herein provided model of T lymphocytes, of their lifecycle and of their interactions with electromagnetic waves provides a consistent interpretation within a single theoretical framework of observed phenomenons which previously were not understood.

This model is viewed as a starting point, evidencing fundamental mechanisms implied in the interaction of T cells with electromagnetic waves. Ideally it should be possible to provide specific chemical formulae of each implied organelle or protein and to provide detailed quantum simulations based on known compounds to confirm the present model in detail, along the lines of what was proposed in [71] for photosynthesis. This is out of reach in the short term, but progress towards this could be one of the targets for further studies. Progressing towards a better understanding of the interactions of the adaptive immune system with electromagnetic waves is expected to imply simultaneous progress on theoretical aspects (the mathematical model), structural aspects (chemical formulae of implied molecules ...), and experimental data (comparable to the experimental data discussed herein, which provides the material base supporting the proposed model).

The most important practical aspect of the present model is the fact that an electromagnetic wave of sufficient bandwidth can affect the immune system at power density levels within the range affecting most of the human population in developed countries. This aspect is reasonably straightforward based on the physical mechanisms implied and it is confirmed by direct epidemiological observation and some unintentional experimental results. It has never been intentionally tested in vitro or in an animal model, yet it should be reasonably easy to test. Due to the practical implications for public health, it is considered that reaching a scientific consensus of this issue should be a priority. This aspect of the model should thus be scrutinized and tested to whatever standard of proof will be required to reach scientific consensus.

The present model also has therapeutic implications. Treatment by electromagnetic waves or by suppression of electromagnetic waves, as the case may be, may become essential in future medical practice. More complex therapeutic applications of the present theory may also emerge.

The experimental data discussed herein comprises a fair share of papers whose authors supported the view that no significant health effects of athermal exposure exist, as well as a fair share of papers whose author's conclusions were prima facie incompatible with each other. Yet with regards to the factual experimental data reported all papers and reports discussed herein, independent of their author's opinions, are consistent and in good agreement with the present theory. The present paper brings in a reasonable scientific explanation for observed phenomenons and shows that experimental data in the field are generally consistent.

References

[1] A.B.H.Bakker, J.H.Phillips, C.G.Figdor, and L.L.Lanier. Killer cell inhibitory receptors for mhc

class i molecules regulate lysis of melanoma cells mediated by nk cells, gamma delta t cells and antigen specific ctl. *J Immunol*, 160:5239–5245, 1998.

[2] Agence Nationale des Fréquences, www.cartoradio.fr, 2012.

[3] L Allais, P Condevaux, P Fant, and P C Barrow. juvenile toxicity of cyclosporin in the rat. *reproductive toxicology*, 28:230–238, 2009.

[4] A J Berteaud, A M Bottreau, A Priore, A N Pautrizel, and F Berlureau. Essai de corrlation entre l'volution d'une affection par trypanosoma equiperdum et l'action d'une onde lectromagntique pulse et module. *Comptes Rendus de l'Acadmie des Sciences de Paris srie D*, 272:1003–1006, 1971.

[5] J P Blanchard and C F Blackman. Clarification of an ion parametric resonance model for magnetic field interactions with biological systems. *Bioelectromagnetics*, 15:217–238, 1994.

[6] R J De Boer and A S Perelson. size and connectivity as emergent properties of a developing immune network. *J. theor. Biol.*, 149:381–424, 1991.

[7] M Bornhausen, J Detlefsen, C Engmann, M Erhard, T Gartner, N Hettenbach, C Kahlfeld, K Kogler, S Okorn, O Petrowicz, S Schelkshorn, J Schneider, J Schreiner, M Shakarami, M Stangassinger, M Stohrer, S Tejero, and C Wohr. Abschlussbericht- forschungsvorhaben des bundesamts fur strahlenschutz- in vivo-experimente unter exposition mit hochfrequenten elektromagnetischen felderns der mobilfunkkommunikation - a langzeituntersuchungen. Technical report, Technische Univetsitat Munchen and Ludwig Maximilians Universitat Munchen, december 2007.

[8] S Budhu, J D Loike, A Pandolfi, S Han, G Catalano, A Constantinescu, R Clynes, and S C. Silverstein. Cd8+ t cell concentration determines their efficiency in killing cognate antigenexpressing syngeneic mammalian cells in vitro and in mouse tissues. *journal of experimental medicine*, 207(1):223–235, 2010.

[9] J Buschmann. Final report: Experimental study on potential interactions of the 3rd generation mobile telecommunication system (umts) with biological systems for the health risk assessment of humans: Two-generation reproduction study in wistar (wu) - rats. Technical report, Fraunhofer Institut - Toxicologie und Experimentelle Medizin, november 2008.

[10] J Buschmann. Final report: Experimental study on potential interactions of the 3rd generation mobile telecommunication systems (umts) with biological systems for the health risk assessment of humans: Developmental neurotoxicity study with umts in wistar (wu) - rats. Technical report, Fraunhofer Institut - Toxicologie und Experimentelle Medizin, february 2009.

[11] *indicateurs de mortalite*. CepiDc-Inserm (Centre d'Epidemiologie sur les Causes Medicales de Deces, Institut National de la Sante et de la Recherche Medicale), www.cepidc.inserm.fr, 2012.

[12] C. Cohen-Tannoudji, B. Diu, and F.Laloe. *Mecanique quantique*. Hermann, 1998.

[13] C N Coleman, T Mason, E P Hooker, and S E Robinson. Developmental effects of intermittent prenatal exposure to 1,1,1- trichloroethane in the rat. *Neurotoxicology and Teratology*, 21(6):699–708, 1999.

[14] E Collini, C Y Wong, K E Wilk, P M G Curmi, P Brumer, and G D Scholes. Coherently wired light-harvesting in photosynthetic marine algae at ambient temperature. *nature*, 463:644–647, 2009.

[15] V L S de Castro and S H Chiorato. Effects of separate and combined exposure to the pesticides methamidophos and chlorothalonil on the development of suckling rats. *International Journal of Hygiene and Environmental Health*, 210:169–176, 2007.

[16] F P de Gannes, M Taxile, S Duleu, A Hurtier, E Haro, M Geffard, G Ruffi, B Billaudel, P Leveque, P Dufour, I Lagroye, and B Veyret. A confirmation study of russian and ukrainian data on effects of 2450 mhz microwave exposure on immunological processes and teratology in rats. *Radiation Research*, 172:617–624, 2009.

[17] J A Dickson and D S Muckle. Total-body hyperthermia versus primary tumor hyperthermia in the treatment of the rabbit vx-2 carcinoma. *Cancer research*, 32:1916–1923, 1972.

[18] H Dolk, G Shaddick, P Walls, C Grundy, B Thakrar, I Kleinschmidt, and P Elliott. Cancer incidence near radio and television transmitters in great britain: Sutton coldfield transmitter. *American Journal of Epidemiology*, 145(1):1–9, january 1997.

[19] H Dolk, G Shaddick, P Walls, B Thakrar, and P Elliott. Cancer incidence near radio and television transmitters in great britain - all high power transmitters. *American Journal of Epidemiology*, 145(1): 10–17, january 1997.

[20] S Dronov and A Kiritseva. Immuno-biological changes in immunized animals after chronic exposure to radiowaves of super-high frequency. *Gigiena i sanitaria*, 7:51–53, 1971. in Russian.

[21] M Ema, S Fuji, M Furukawa, M Kiguchi, T Ikka, and A Harazono. Rats two-generation reproductive toxicity study of bisphenol a. *reproductive toxicology*, 15:505–523, 2001.

[22] M Ema, S Fuji, M Matsumoto, M Hirata-Koizumi, A Hirose, and E Kamata. two-generation reproductive toxicity study of the rubber accelerator n,n dicyclohexyl-3-benzothiazolesulfamide in rats. *reproductive toxicology*, 25:21–38, 2008.

[23] G S Engel, T R Calhoun, E L Read, T-K Ahn, T Man, Y-C Cheng, and G R Blankenship, R E andFleming. Evidence for wavelike energy transfer through quantum coherence in photosynthetic systems. *nature*, 446:782–786, 2007.

[24] E E Fesenko, V R Makar, E G Novoselova, and V B Sadovnikov. Microwaves and cellular immunity i. effect of whole body microwave irradiation on tumor necrosis factor in mouse cells. *biochemistry and bioenergetics*, 49:29–35, 1999.

[25] S Fuji, K Yabe, M Furukawa, M Matsuura, and H Aoyama. A one-generational reproductive toxicity study of ethyl tertiary butyl ether in rats. *Reproductive Toxicology*, 30:414–421, 2010.

[26] E M Gauger, E Rieper, J J L Morton, S C Benjamin, and V Vedral. Sustained quantum coherence and entanglement in the avian compass. *Physical Review Letters*, 106:040503, 2011.

[27] Y Grigoriev. Bioinitiative report: a rationale for a biologically-based public exposure standard for electromagnetic fields (elf and rf). section 8 - supplement. Technical report, Bioinitiative Working Group, 2012.

[28] Y G Grigoriev, A. A. Ivanov, V. N. Maltsev, A. M. Ulanova, N. M. Stavrakova, I. A. Nikolaeva, and O. A. Grigoriev. Autoimmune processes after long-term low-level exposure to electromagnetic fields (experimental results) part 4. oxidative intracellular stress response to the long-term rat exposure to nonthermal rf emf. *Biophysics*, 55(6):1054–1058, 2010. ISSN 0006-3509. doi: 10.1134/S000635091006031X.

[29] Yury G Grigoriev, Oleg A Grigoriev, A A Ivanov, A M Lyaginskaya, A V Merkulov, N B Shagina, V N Maltsev, P Leveque, d V A Osipov A M Ulanova a, and A V Shafirkin. Confirmation studies of soviet research on immunological effects of microwaves: Russian immunological results. *Bioelectromagnetics*, 31: 589–602, 2010.

[30] T Hagao, K Wada, M Kuwagata, and H Ono. Effects of prenatal and postnatal exposure to styrene dimers and trimers on reproductive function in rats. *Reproductive Toxicology*, 14:403–415, 2000.

[31] O Hallberg and O Johansson. Increasing melanoma - too many skin cell damages or too few repairs ? *Cancers*, 5:184–204, 2013.

[32] L Hardell, M Carlberg, F Soderqvist, and K Hansson Mild. Case-control study of the association between malignant brain tumors diagnosed between 2007 and 2009 and mobile and cordless phone use. *international journal of oncology*, September 2013. doi: 10.3892/ijo.2013.2111.

[33] E Heuland, M A Germaux, L Galineau, S Chalon, and C Belzung. prenatal mdma exposure delays postnatal development in the rat: A preliminary study. *Neurotoxicology and Teratology*, 32:425–431, 2010.

[34] M Hirata-Koizumi, S Fuji, A Ono, A Hirose, T Imai, K Ogawa, and A Nishikawa. Two-generation reproductive study of aluminium sulfate in rats. *reproductive toxicology*, 2010.

[35] L J Hushka, S J Waterman, L H Keller, G W Trimmer, J J Freeman, J L Ambroso, M Nicolich, and R H McKee. two-generation reproduction studies in rats fed di-isodecyl phtalate. *reproductive toxicology*, 15: 153–169, 2001.

[36] I.Carena, A. Shamshiev, A. Donda, M. Colonna, and G.D. Libero. Major histocompatibility complex class i molecules modulate activation threshold and early signaling of t cell antigen receptor-gama/delta stimulated by nonpeptidic ligands. *J. Exp. Med.*, 186(10): 1769–74, November 1997.

[37] H. Ikeda, B. Leth, F.Lehmann, N.V.Baren, J.F.Baurain, C. D. Smet, H. Chambost, M.Vitale, A. Moretta, T. Boon, and P.G.Coulie. Characterization of an antigen that is recognized on a melanoma showing partial hla loss by ctl expressing an nk inhibitory receptor. *Immunity*, 6:199–208, february 1997.

[38] P D Inskip, R E Tarone, E E Hatch, and P D Timothy et al. cellular-telephone use and brain tumors. *The New England Journal of Medicine*, 344(2):79–86, january 2001.

[39] Study Group Interphone. Brain tumour risk in relation to mobile telephone use: results of the interphone international case-control study. *International Journal of Epidemiology*, 39:675–694, 2010.

[40] C Johansen, J D Boice, J K McLaughlin, and J H Olsen. Cellular telephones and cancer: a nationwide cohort study in denmark. *Journal of the National Cancer Institute*, 93(3):203–206, february 2001.

[41] O F Johnson, E T Gilbreath, T C Graham, and S Gorham. Reproductive and developmental toxicities of zinc supplemented rats. *reproductive toxicology*, 2010.

[42] J.V.Ravetch and L.L.Lanier. Immune inhibitory receptors. *Science*, 290(5489):84–89, 2000.

[43] Y Katakura, R Kishi, T Ikeda, and H Miyake. Effects of prenatal styrene exposure on postnatal development and brain serotonin and catecholamine levels in rats. *Environmental Research section A*, 85:41–47, 2001.

[44] I K Kominis. quantum zeno effect explains magnetic-sensitive radical-ion-pair reactions. *Physical Review E*, 80:056115, 2009.

[45] A Lakhola, A Auvinen, M J Schoemaker, H C Christensen, M Feychting, C Johansen, L Klaeboe, A J Swerdlow, T Tynes, and T Salminen. Mobile phone use and risk of glioma in 5 north european countries. *International Journal of Cancer*, 120:1769–1775, 2007.

[46] G Lakhovsky. Appareil destiné a la création de champs électriques de haute fréquence a longueurs d'ondes multiples, 1932. patent number FR 732.276.

[47] Georges Lakhovsky. *Radiations and Waves, Sources of Our Life*. Emile L Cabella, 288 East 45th Street, New York, 1941.

[48] Vincent Lauer. A Quantum Theory of the Biological Effects of Radio-frequencies and its application to Cancer. Oct 2013. URL `http://hal.archives-ouvertes.fr/hal-00877298`.

[49] V V Lednev. Possible mechanism for the influence of weak magnetic fields on biological systems. *Bioelectromagnetics*, 12:71–75, 1991.

[50] A Lerchl. Abschlussbericht fur das forschungsvorhaben: Langzeitstudie an labornagern mit umts-signalen. Technical report, Jacobs University Bremen, january 2008.

[51] Y Li, M Zhuang, T Li, and N Shi. Neurobehavioral toxicity study of dibutyl phtalate on rats following in utero and lactational exposure. *journal of applied toxicology*, 29:603–611, 2009.

[52] D B Lyle, P Schechter, W R Adey, and R L Lundak. Suppression of t-lymphocyte cytotoxicity following exposure to sinusoidally amplitude-modulated fields. *bioelectromagnetics*, 4:281–292, 1983.

[53] H R Macdonald. Effect of hyperthermia on the functional activity of cytotoxic t-lymphocytes. *journal of the national cancer institute*, 59(4), 1977.

[54] T A Mace, L Zhong, K M Kokulus, and E A Repasky. Effector cd8+ t cell ifn-gamma and cytotoxicity are enhanced by mild hyperthermia. *Int J Hyperthermia*, 28(1):9–18, 2012.

[55] M.Coltey, R.P.Bucy, C.H.Chen, J.Chiak, U.Losch, D.Char, N.M.Le Douarin, and M.D.Cooper. Analysis of the first two waves of thymus homing stem cells and their t cell progeny in chick-quail chimeras. *J. Exp. Med.*, 170:543–57, 1989.

[56] C. E. Moody, J. B. Innes, L. Staiano-Coico, G.S. Incefy, H. T. Thaler, and M.E. Weksler. Lymphocyte transformation induced by autologous cells xi. the effect of age on the autologous mixed lymphocyte reaction. *Immunology*, 44:431–438, 1981.

[57] M.O.Scully and M. Suhail Zubairy. *Quantum optics*. Cambridge university press, 1997.

[58] J E Muscat, M G Malkin, S Thompson, S D Stellman, D McRee, A I Neugut, and E L Wynder. Handheld cellular telephone use and risk of brain cancer. *JAMA*, 284(23):3001–3007, December 2000.

[59] T Nagao, R Ohta, H Marumo, T Shindo, S Yoshimura, and H Ono. Effect of butyl benzyl phtalate in sprague-dawley rats after gavage administration: a two-generation reproductive study. *reproductive toxicology*, 14:513–532, 2000.

[60] T Nagao, K Wada, H Marumo, S Yoshimura, and H Ono. Reproductive effects of nonylphenom in rats after gavage administration: a two-generation study. *Reproductive Toxicology*, 15:293–315, 2001.

[61] H Ndoumbe Mbonjo Mbonjo, J Streckert, A Bitz, V Hansen, A Glasmachers, S Gencol, and D Rozic. Generic umts test signal for rf bioelectromagnetic studies. *bioelectromagnetics*, 25:415–425, 2004.

[62] H Ozyurek, A Bozkurt, S Bilge, E Ciftcioglu, F Ilkaya, and D B Bas. effects of prenatal levetiracetam exposure on motor and cognitive functions of rat offspring. *Brain and development*, 32:396–403, 2010.

[63] J L Portes. *la vie et l'oeuvre de Georges Lakhovsky*. PhD thesis, Université Pierre et Marie Curie - facult de mdecine Piti-Salptrire, 1983.

[64] A Priore. Dispositif pour la production d'un rayonnement biologiquement actif, 1966. patent number FR 1.501.984.

[65] M Repacholi, Y Grigoriev, J Buschmann, and C. Pioli. Scientific basis for the soviet and russian radiofrequency standards for the general public. *bioelectromagnetics*, 2012.

[66] M H Repacholi, A Basten, V Gebski, D Noonan, J Finnie, and A W Harris. Lymphomas in emupim1 transgenic mice exposed to pulsed 900 mhz electromagnetic fields. *Radiation Research*, 147:631–640, 1997.

[67] M-R Riviere, A Priore, F Berlureau, M Fournier, and M Gurin. Action de champs lectromagntiques sur les greffes de la tumeur t8 chez le rat. *Comptes Rendus de l'Acadmie des Sciences de Paris*, 259:4895–4897, 1964.

[68] W Roszkowski, J K Wrembel, R Roszkowski, M Janiak, and S Szmigielski. Does whole-body hyperthermia therapy involve participation of the immune system ? *International Journal of Cancer*, 25:289, 1980.

[69] B. Sacco and T. Kerselaers. *The Lakhovsky Multiple Wave Oscillator Secrets Revealed*. 2011. http://users.skynet.be/Lakhovsky.

[70] F Salvatori, C B Talassi, S A Salzgeber, H S Spinosa, and M M Bernardi. Embryotoxic and long-term effects of cadmium exposure during embryogenesis in rats. *Neurotoxicology and Teratology*, 26:673–680, 2004.

[71] M Sarovar, A Ishizaki, G R Fleming, and K B Whaley. Quantum entanglement in photosynthetic light-harvesting complexes. *Nature Physics*, 6:462–467, 2010.

[72] J. Schuz, R Jacobsen, J H Olsen, J D Boice Jr, J K McLaughlin, and C Johansen. Cellular use and cancer risk: Update of a nationwide danish cohort. *Journal of the National Cancer Institute*, 98(23):1707–1713, december 2006.

[73] W H Siddiqui, D G Stump, K P Plotzke, J F Holson, and R G Meeks. A two-generation reproductive toxicity study of octamethylcyclotetrasiloxane (d4) in rats exposed by whole-body vapor inhalation. *Reproductive Toxicology*, 23:202–215, 2007.

[74] W H Siddiqui, D G Stump, V L Reynolds, K P Plotzke, J F Holson, and R G Meeks. A two-generation reproductive toxicity study of decamethylcyclopentasiloxane (d5) in rats exposed by whole-body vapor inhalation. *Reproductive Toxicology*, 23: 216–225, 2007.

[75] J B Smith, R P Knowlton, and S S Agarwal. Human lymphocyte responses are enhanced by culture at 40 c. *the journal of Immunology*, 121(2):691–694, 1978.

[76] A M Sommer, K Grote, T Reinhardt, J Streckert, V Hansen, and A Lerchl. Effects of radiofrequency electromagnetic fields (umts) on reproduction and development of mice: a multi-generation study. *radiation research*, 171:89–95, 2009.

[77] S Szmigielski. reaction of the immune system to low-level rf/mw exposures. *Science of the Total Environment*, 454-455:393–400, 2013.

[78] A Szudinski, A Pietraszek, M Janiak, J Wrembel, M Kalczak, and S Szmigielski. Acceleration of the development of benzopyrene-induced skin cancer in mice by microwave radiation. *Archives of Dermatological Research*, 274:303–312, 1982.

[79] S Takahashi, N Imai, K Nabae, K Wake, H Kawai, J Wang, S Watanabe, M Kawabe, O Fujiwara, K Ogawa, S Tamano, and T Shirai. Lack of adverse effects of whole-body exposure to a mobile telecommunication electromagnetic field on the rat fetus. *Radiation Research*, pages 362–372, 2010.

[80] C Tanchot, F A Lemonnier, B Pérarnau, A A Freitas, and B Rocha. Differential requirements for survival and proliferation of cd8 naive or memory t cells. *science*, 276(5321):2057–2062, 1997. doi: 10.126/science.276.5321.2057.

[81] R Thiel and I Chahoud. Postnatal development and behaviour of wistar rats after prenatal toluene exposure. *Arch. Toxicol.*, 71:238–265, 1997.

[82] D F Tough and J Sprent. Lifespan of gamma/delta t cells. *Journal of Experimental Medicine*, 187(3), 1998.

[83] R W Tyl, C B Myers, M C Marr, N P Castillo, M M Veselica, R L Joiner, S S Dimond, J P Van Miller, G D Stropp, J M Waechter, and S G Hentges. One-generation reproductive toxicity study of dietary 17-beta estradiol (e2; cas no 50-28-2) in cd-1 (swiss)mice. *reproductive toxicology*, 25:144–160, 2008.

[84] B Veyret, C Bouthet, P Deschaux, R de Seze, M Geffard, J Joussot-Dubien, M le Diraison, J M Moreau, and A Caristan. Antibody responses of mice exposed to low-power microwaves unde combined pulse-and-amplitude modulation. *Bioelectromagnetics*, 12:47–56, 1991.

[85] G I Vinogradov and Y D Dumanski. About ther sensitizing effect of electromagnetic fields of ultra-high frequency. *Gig. Sanit.*, 9:31–35, 1975.

[86] C R Willoughby, S M Fulcher, D M Creasy, J A Heath, R A J Priston, and N P Moore. Two-generation reproduction toxicity studies of di-(c7-c9 alkyl) phtalate and di-(c9-c11 alkyl) phtalate in the rat. *Reproductive Toxicology*, 14:427–450, 2000.

[87] R Wolf and D Wolf. Increased incidence of cancer near a cell-phone transmitter station. *International Journal of Cancer Prevention*, 1(2), april 2004.

Appendices

A Calculation of transition probabilities between two conformations

In this section I discuss transition probabilities between two conformations of an elementary biological system, which in the present case includes at least the TCR-pMHC system.

I model the elementary biological system using a set of coordinates typically representing atom positions, ignoring electronic transitions. This approach is generally accepted for modelling vibrational levels of molecules, see for example the ammonia molecule in [12]. Ignoring electronic transitions is acceptable because electronic transitions generally correspond to energy differences significantly higher than vibrational energy differences or conformational energy differences.

Figure 11 shows a schematic representation of the energy variations of an elementary biological system, in a single-dimensional case. The vertical axis represents the energy $\mathscr{E}$, the horizontal axis represents a coordinate x. The curved line represents the conformational energy of the elementary biological system as a function of x. Although I represented a single degree of liberty x, this model in the general case has a plurality of degrees of liberty which I shall describe as a vector $\mathbf{x}$ in an s-dimensional coordinate space S. For example, a component of $\mathbf{x}$ can be a distance between two atoms of the elementary biological system or an angle between two parts of the elementary biological system which can rotate relative to each other.

The energy of the elementary biological system has two wells (a) and (b) respectively centred at $\mathbf{x}_a$ and $\mathbf{x}_b$. These wells correspond to distinct configurations (a) and (b) of the elementary biological system, respectively. In configuration (a) [resp. (b)] the wave function of the elementary biological system essentially has its non-zero values around x_a [resp. x_b], inside a bound portion I_a [resp. I_b] of the s-dimensional coordinate space S (in the one-dimensional case I_a and I_b are intervals).

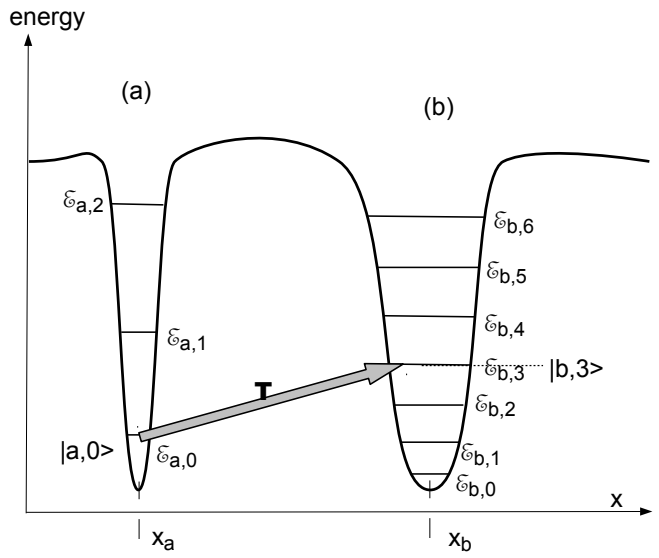

Figure 11: energy profile showing two quantum wells.

In the represented one-dimensional case the quantum state of the elementary biological system in the potential well (a) may be any of the ground state $|a,0\rangle$ (having energy $\mathscr{E}_{a,0}$) or the first excited state $|a,1\rangle$ (having energy $\mathscr{E}_{a,1}$) or the second excited state $|a,2\rangle$(having energy $\mathscr{E}_{a,2}$). Each of these states represents a different vibrational level of the elementary biological system in well (a), and has been represented as a horizontal bar inside well (a), at a vertical position corresponding to its energy. Generally, I will note $|a,n\rangle$ [resp. $|b,n\rangle$] the n-th excited state (with $n=0$ for the ground state) of the elementary biological system in quantum well (a) [resp. (b)] and $\mathscr{E}_{a,n}$ [resp. $\mathscr{E}_{b,n}$] the energy of the elementary biological system in that quantum state.

If wells (a) and (b) were limited by infinitely high potential barriers, then an eigenfunction of the elementary biological system would be entirely within well (a) and another eigenfunction would be entirely within well (b). If the potential barriers have finite height, then assuming the energy levels in well (b) are different from the energy levels in well (a) (i.e. assuming that $\mathscr{E}_{a,n} \neq \mathscr{E}_{b,m}$ for all useful values of n, m) the finiteness of the potential barrier acts as a perturbation of each eigenfunction, so that the eigenfunctions $|a,n\rangle$ remain essentially unchanged within potential well (a) but acquire very small component in potential well (b). This small component is not an eigenfunction in potential well (b) and therefore there are at least some eigenfunctions in potential well (b) to which ones the small component is not orthogonal. As a result of this, the overlap

$$O_{a,n;b,m} = \int\limits_{(I_a)} \phi_{a,n}(\mathbf{x})\phi^*_{b,m}(\mathbf{x})\,\mathrm{d}\mathbf{x} \tag{19}$$

is small but non-zero for at least some couples of eigenfunctions $|a,n\rangle$, $|b,m\rangle$ wherein $\mathscr{E}_{a,n} \neq \mathscr{E}_{b,m}$, with $\phi_{a,n}(\mathbf{x}) = \langle \mathbf{x}|a,n\rangle$, $\phi_{b,m}(\mathbf{x}) = \langle \mathbf{x}|b,m\rangle$.

Now I assume that the elementary biological system when in the configuration (a) [resp. (b)] has a (three-dimensional) electric dipole moment $\mathbf{d}(\mathbf{x}) = \mathbf{d}_a$ [resp. $\mathbf{d}(\mathbf{x}) = \mathbf{d}_b$] which is substantially constant over I_a [resp. I_b]. I also assume that the probability of presence $\langle \phi_{a,n}(\mathbf{x})|\phi_{a,n}(\mathbf{x})\rangle$ [resp. $\langle \phi_{b,m}(\mathbf{x})|\phi_{b,m}(\mathbf{x})\rangle$] is essentially concentrated in I_a [resp. I_b] with other non-zero values in I_b [resp. I_a] and is negligible everywhere else. Then:

$$\int\limits_{(S)} \phi_{a,n}(\mathbf{x})\phi^*_{b,m}(\mathbf{x})\,\mathrm{d}^s\mathbf{x} = \int\limits_{(I_a)} \phi_{a,n}(\mathbf{x})\phi^*_{b,m}(\mathbf{x})\,\mathrm{d}^s\mathbf{x} + \int\limits_{(I_b)} \phi_{a,n}(\mathbf{x})\phi^*_{b,m}(\mathbf{x})\,\mathrm{d}^s\mathbf{x} = 0 \tag{20}$$

wherein the equality to zero is due to $|a,n\rangle$ and $|b,m\rangle$ being mutually orthogonal eigenfunctions.
and:

$$\int\limits_{S} \phi_{a,n}(\mathbf{x})\mathbf{d}(\mathbf{x})\phi^*_{b,m}(\mathbf{x})\,\mathrm{d}^s\mathbf{x} = \mathbf{d}_a \int\limits_{I_a} \phi_{a,n}(\mathbf{x})\phi^*_{b,m}(x)\,\mathrm{d}^s\mathbf{x} + \mathbf{d}_b \int\limits_{I_b} \phi_{a,n}(\mathbf{x})\phi^*_{b,m}(\mathbf{x})\,\mathrm{d}^s\mathbf{x} \tag{21}$$

Combining equations 20 and 21 yields the three-dimensional electric dipole matrix element:

$$\mathbf{D}_{a,n;b,m} = \langle \phi_{a,n}|\mathbf{d}|\phi_{b,m}\rangle = \int\limits_{(S)} \phi_{a,n}(\mathbf{x})\mathbf{d}(\mathbf{x})\phi^*_{b,m}(\mathbf{x})\,\mathrm{d}^s\mathbf{x} = (\mathbf{d}_a - \mathbf{d}_b) \int\limits_{(I_a)} \phi_{a,n}(\mathbf{x})\phi^*_{b,m}(\mathbf{x})\,\mathrm{d}^s\mathbf{x} \tag{22}$$

Which can be written using the definition in equation (19):

$$\mathbf{D}_{a,n;b,m} = (\mathbf{d}_a - \mathbf{d}_b)O_{a,n;b,m} \tag{23}$$

The individual components of this dipole matrix element are the matrix elements of the projections of the dipole moment on each axis.

The dipole matrix element $\mathbf{D}_{a,n;b,m}$ between the eigenstates $|a,n\rangle$ and $|b,m\rangle$ is thus proportional to the difference between the dipole moments in each conformation, and to the overlap on a single quantum well between the two eigenstate wave functions. When the overlap is non-zero and there is a difference between the elementary biological system's dipole moments in each conformation, then there will be a non-zero transition dipole matrix element and thus a transition between the two eigenstates $|a,n\rangle$ and $|b,m\rangle$ is allowed which can yield stimulated transitions when the elementary biological system is exposed to an electromagnetic field of frequency $\nu = \frac{1}{h}|\mathscr{E}_{a,n} - \mathscr{E}_{b,m}|$. An example of an allowed transition from $|\phi_{a,0}\rangle$ to $|\phi_{b,3}\rangle$ is represented on figure 11 as T. This transition brings the elementary biological system from configuration (a) to configuration (b) despite the existence of the potential barrier, in a manner analogous to the quantum tunneling effect.

When the elementary biological system is submitted to a time-varying electric field $\mathbf{E}\cos\omega t$ the matrix element of

the interaction hamiltonian between the elementary biological system and the field is :

$$\langle a,n|H_{int}|b,m\rangle = \mathbf{D}_{a,n;b,m}\cdot\mathbf{E}\cos\omega t \tag{24}$$

wherein $\cdot$ denotes the scalar product.

When interacting with the field the elementary biological element undergoes Rabi oscillations between states $|a,n\rangle$ and $|b,m\rangle$ and the frequency of these transitions is the Rabi frequency

$$\Omega_{a,n;b,m} = \frac{1}{\hbar}\mathbf{E}\cdot\mathbf{D}_{a,n;b,m} \tag{25}$$

This equation may also be written:

$$\Omega_{a,n;b,m} = \frac{1}{\hbar}\mathbf{E}\cdot(\mathbf{d}_a-\mathbf{d}_b)O_{a,n;b,m} \tag{26}$$

B Equivalent RMS Rabi frequencies

Rabi frequencies governing transitions stimulated by the electromagnetic field are usually defined for single mode electromagnetic waves. However, electromagnetic waves which are not single mode can also cause stimulated transitions between quantum states. In this section I discuss a simple approximation which facilitates the evaluation of transitions stimulated by electromagnetic waves which have an extended frequency spectrum. This approximation is based on the use of equivalent Rabi frequencies which have the same role which Rabi frequencies have for single mode waves.

B.1 single mode frequency range

I first consider only a single mode electromagnetic wave with a frequency shift $\Delta\omega$ with respect to the resonance of an $|a\rangle$ to $|b\rangle$ transition between wells (a) and (b) (for simplicity I now omit the indexation of the energy states within each quantum well). The Rabi frequency of the $|a\rangle$ to $|b\rangle$ transition for the electric field amplitude of this single mode wave is Ω_S. The inversion (probability of finding the system in state $|a\rangle$ minus probability of finding the system in state $|b\rangle$) is (see for example section 5.2 of [57]) : $\frac{(\Delta\omega)^2-\Omega_S^2}{(\Delta\omega)^2+\Omega_S^2}\sin^2\left(\frac{1}{2}\sqrt{(\Delta\omega)^2+\Omega_S^2}\right)+\cos^2\left(\frac{1}{2}\sqrt{(\Delta\omega)^2+\Omega_S^2}\right)$ which can also be written $\frac{(\Delta\omega)^2}{(\Delta\omega)^2+\Omega_S^2}+\frac{\Omega_S^2}{(\Delta\omega)^2+\Omega_S^2}\cos(\sqrt{(\Delta\omega)^2+\Omega_S^2})$. The amplitude of the variable part is $\frac{\Omega_S^2}{(\Delta\omega)^2+\Omega_S^2}$. The full width at half maximum (FWHM) of this amplitude as a function of $\Delta\omega$ is $2\Omega_S$. In a first approximation, the only frequencies that contribute to stimulated absorption and emission are thus within a frequency range of $2\Omega_S$.

B.2 equivalent Rabi frequency and Rabi integration bandwidth

Now I consider an electromagnetic wave which is a flat Gaussian noise having a spectral power density S_{tot} near the resonant frequency of the $|a\rangle$ to $|b\rangle$ transition, and which electric field is parallel to the three-dimensional electric dipole matrix element $\mathbf{D}_{a;b}$ corresponding to the $|a\rangle$ to $|b\rangle$ transition.

The RMS value E_{tot} of the electric field in a small angular frequency range $\delta\omega$ centred on the resonant frequency of the $|a\rangle$ to $|b\rangle$ transition is related to the bandwidth and spectral power density by:

$$S_{tot}\frac{\delta\omega}{2\pi} = \frac{E_{tot}^2}{c\mu_0} \tag{27}$$

The RMS Rabi frequency of the $|a\rangle$ to $|b\rangle$ transition for a field E_{tot} parallel to $\mathbf{D}_{a;b}$ is, from equation 25:

$$\Omega_{tot} = \frac{1}{\hbar}D_{ab}E_{tot} \tag{28}$$

with $D_{ab} = |\mathbf{D}_{a;b}|$.

In a simple approximation, only a central frequency slot of the electromagnetic wave centred on the resonant frequency of the $|a\rangle$ to $|b\rangle$ transition, has a significant role in $|a\rangle$ to $|b\rangle$ stimulated transitions. The bandwidth of this frequency slot is a "Rabi integration bandwidth" $\delta\omega$ corresponding to the frequency range $2\Omega_S$ obtained in section B.1, in which Ω_{tot} now replaces Ω_S:

$$\delta\omega = 2\Omega_{tot} \tag{29}$$

This bandwidth is also equal to the bandwidth on which the spectral power density is integrated in equation 27 for the purpose of obtaining the RMS Rabi frequency Ω_{tot}, so that equations 27, 28 and 29 can be combined, yielding:

$$\Omega_{tot} = 2\mu_0 c\frac{D_{ab}^2}{\hbar^2}\frac{S_{tot}}{2\pi} \tag{30}$$

The RMS Rabi frequency of the $|a\rangle$ to $|b\rangle$ transition for the part of the electric field which stimulates $|a\rangle$ to $|b\rangle$ transitions ("equivalent RMS Rabi frequency") is thus given by equation 30. This approximation is only valid when the Rabi integration bandwidth - which is twice the Rabi frequency as per equation 29 - remains small compared to the overall bandwidth of the electromagnetic wave.

B.3 thermally stimulated transitions

The effects of artificial electromagnetic waves on transitions between quantum states of the elementary biological system must be compared to the likelihood of such transitions occurring naturally. Such transitions may occur naturally by spontaneous decay or because the thermal electromagnetic field stimulates transitions.

From Planck's law the thermal spectral power density, or power per unit area in a solid angle corresponding to a half space and in a frequency range $\frac{\delta\omega}{2\pi}$ around the center frequency $\frac{\omega}{2\pi}$, is (for small ω):

$$S_{th} = \frac{1}{(2\pi)}\frac{\omega^2}{c^2}kT \tag{31}$$

wherein k is Boltzmann's constant, T is the temperature in Kelvins.

The RMS value E_{th} of the thermal electric field along an arbitrary direction in a frequency range $\delta\omega$ is related to the thermal spectral power density per unit area by:

$$S_{th}\frac{\delta\omega}{2\pi} = \frac{E_{th}^2}{c\mu_0} \tag{32}$$

Equation 32 corresponds to equation 27 and the equivalent Rabi frequency (or thermal Rabi frequency Ω_{th})can thus be obtained by substituting S_{th} to S_{tot} in equation 30 yielding:

$$\Omega_{th} = 2\frac{1}{(2\pi)^2}c\mu_0 kT\left(\frac{\omega D_{ab}}{\hbar c}\right)^2 \tag{33}$$

B.4 artificial wave superimposed on the thermal electric field

I assume that an artificial electromagnetic wave superimposed on the thermal electric field has an electric field parallel to the three-dimensional electric dipole matrix element $\mathbf{D}_{a;b}$. In this case the equivalent Rabi frequency is obtained by substituting $S_{art}+S_{th}$ in equation 30, wherein S_{art} is the spectral power density of the artificial wave, yielding:

$$\Omega_{tot} = 2\mu_0 c\frac{D_{ab}^2}{\hbar^2}\frac{S_{art}+S_{th}}{2\pi} \tag{34}$$

B.5 dominance of thermally stimulated transitions over spontaneous decay

I will momentarily use a thermal bandwidth Γ_{th} which is the inverse of the lifetime of an initial pure state (a or b) and is thus one quarter of the equivalent RMS Rabi frequency:

$$\Gamma_{th} = \frac{2}{4(2\pi)^3}c\mu_0 kT\left(\frac{\omega D_{ab}}{\hbar c}\right)^2 \tag{35}$$

This thermal bandwidth compares with the spontaneous decay bandwidth which is [57]:

$$\Gamma_{spont} = \frac{\omega^3 D_{ab}^2}{3\pi\epsilon_0 c^3\hbar} \tag{36}$$

I can thus calculate

$$\frac{\Gamma_{spont}}{\Gamma_{th}} = \frac{4(2\pi)^2}{3}\frac{1}{\mu_0\epsilon_0 c^2}\frac{\hbar\omega}{kT} \tag{37}$$

This value is 1 when the angular frequency ω is :

$$\omega_{trans} = \frac{3}{4(2\pi)^2}\mu_0\epsilon_0 c^2\frac{kT}{\hbar} \tag{38}$$

$\frac{\omega_{trans}}{2\pi}$ is about 120 GHz. Below this, stimulated thermal emission - absorption between a higher energy state and a lower energy state dominate over spontaneous decay from the higher energy to the lower energy state. This is the case for all radiofrequencies of interest. Therefore spontaneous decay will generally be ignored herein and transition probabilities will be calculated based on stimulated transitions only.

C statistical methods for evaluating yearly statistics

The statistics in section 3.1.9 concern yearly numbers of deaths due to a specific cause in a specific age category. The question of interest is whether a year's figure is significantly high relative to the previous years. This question is slightly unusual in epidemiology: usually a sample of interest is compared to a reference sample corresponding to the same time period. It is thus necessary to evaluate the significance of figures using a specific method. For estimating the significance of these figures the following procedure is followed:

- an estimate of the number of expected yearly deaths is computed based on the N previous years as

$$\lambda_N(y) = \frac{pop(y)}{N}\left(\frac{De(y-1)}{pop(y-1)} + \frac{De(y-2)}{pop(y-2)} \cdots + \frac{De(y-N)}{pop(y-N)}\right) \tag{39}$$

wherein $pop(y)$ is the population basis on which the number of deaths $De(y)$ is considered (for example, $pop(y)$ is the number of men in the 35-44 age range and $De(y)$ is the number of deaths by cancer in the same age range). When the population is unknown or not used, a constant value of $pop(y)$ is used in the equations.

- The probability of each integer number of deaths k occurring in the 35-44 age category is calculated by applying a Poisson law (which applies because each death is considered independent from the other and the population basis from which the number of deaths is extracted is large):

$$P_N(y,k) = e^{\lambda_N(y)}\frac{\lambda_N(y)^k}{k!} \tag{40}$$

- The probability of the number of deaths in the age class 35-54 being more than or equal to the number $De(y)$ of deaths actually observed is calculated as

$$P_{+,N}(y) = 1 - \sum_{k=0}^{De(y)-1} P_N(y,k). \tag{41}$$

- $P_{+,N}(y)$ sometimes depend strongly on N. To avoid considering a result as significant where it is significant only for a specific value of N, the maximum value over $N = 1$ to 6 of the above probability is calculated:

$$P_+(y) = \max_{N=1\cdots 6} P_{+,N}(y) \tag{42}$$

- An increase of the number of deaths is considered significant when $P_+(y) < 0.05$.